



**MONTCLAIR STATE**  
UNIVERSITY

Montclair State University  
**Montclair State University Digital  
Commons**

---

Theses, Dissertations and Culminating Projects

---

1-2025

## Quantifying the vulnerability of smooth dogfish and winter skate to electromagnetic fields from offshore wind transmission cables in the mid-Atlantic shelf

Rachel A. Sechrist  
*Montclair State University*

Follow this and additional works at: <https://digitalcommons.montclair.edu/etd>



Part of the [Biology Commons](#), [Marine Biology Commons](#), and the [Oil, Gas, and Energy Commons](#)

---

### Recommended Citation

Sechrist, Rachel A., "Quantifying the vulnerability of smooth dogfish and winter skate to electromagnetic fields from offshore wind transmission cables in the mid-Atlantic shelf" (2025). *Theses, Dissertations and Culminating Projects*. 1460.

<https://digitalcommons.montclair.edu/etd/1460>

This Thesis is brought to you for free and open access by Montclair State University Digital Commons. It has been accepted for inclusion in Theses, Dissertations and Culminating Projects by an authorized administrator of Montclair State University Digital Commons. For more information, please contact [digitalcommons@montclair.edu](mailto:digitalcommons@montclair.edu).

## ABSTRACT

The development of offshore wind structures in the northeastern U.S. will contribute to renewable energy goals, but will overlap with many marine species as well as economically important fisheries. High voltage transmission cables from offshore wind farms emit electromagnetic fields (EMFs) that elasmobranchs may detect using sensory organs known as ampullae of Lorenzini. However, sensitivity to EMFs varies by species due to differences in the number and arrangement of pores, the length of subdermal canals within the ampullae of Lorenzini sensory network, and the habitats they reside and regions they forage. For species who reside or forage in benthic regions, exposure potential to EMFs may be substantially higher than pelagic species due to proximity to the cables. This study quantified the vulnerability of two economically important elasmobranch species, smooth dogfish (*Mustelus canis*) and winter skate (*Leucoraja ocellata*), as a function of physiological sensitivity to electromagnetic fields and spatial exposure to the cables. The first ampullary pore maps were constructed for both species in order to better understand their potential sensitivity to EMFs. Using GIS, cable routes from offshore wind farms were overlaid with winter skate and smooth dogfish distributions to quantify: 1) the footprint of the transmission cables from each of the region's offshore wind projects that overlaps with habitat of either species and 2) the proportion of both species' geographic range within the study area that is potentially impacted by offshore wind development. Pore counts ranging from 1052 to 1924 indicate that *M. canis* has a relatively high resolution electrosensory system compared to other Carcharhiniformes. An average pore count of 476 in *L. ocellata* indicates a lower resolution. Offshore wind cable placement off the coasts of New York, Rhode Island, and Massachusetts are within regions of high biomass for both species. Nearly 27% of fall 2015-2019 *M. canis* distribution was intersected by offshore wind

transmission cables, indicating the species is likely at high risk for direct effects from EMFs. Spring and fall *L. ocellata* exposure is lower at 10% and 8% respectively, but proximity to the benthos suggests that true exposure to EMFs is likely higher than that of *M. canis*. Based on pore maps and GIS analyses, *M. canis* has both high sensitivity to electric fields and high exposure to OWF transmission cables, and *L. ocellata* has low sensitivity and high exposure.

MONTCLAIR STATE UNIVERSITY

Quantifying the vulnerability of smooth dogfish and winter skate to electromagnetic fields from  
offshore wind transmission cables in the mid-Atlantic shelf

By

Rachel A. Sechrist

A Master's Thesis Submitted to the Faculty of Montclair State University

In Partial Fulfillment of the Requirements

For the Degree of


Master of Science

January 2025


College of Science and Mathematics

Department of Biology

Thesis Committee:

  
Paul A. X. Bologna

  
Tobey Curtis

  
Matthew Schuler

  
Kyle Newton

QUANTIFYING THE VULNERABILITY OF SMOOTH DOGFISH AND WINTER SKATE  
TO ELECTROMAGNETIC FIELDS FROM OFFSHORE WIND TRANSMISSION CABLES  
IN THE MID-ATLANTIC SHELF

A THESIS

Submitted in partial fulfillment of the requirements

For the degree of Master of Science

Marine Biology and Coastal Sciences

By

Rachel A. Sechrist

Montclair State University

Montclair, NJ

2025

## **ACKNOWLEDGEMENTS**

I would like to dedicate this thesis to my parents who never failed to support me. You are the reason that I never doubted my dream of becoming a marine scientist. It is thanks to you that I fell in love with nature, science, and everything weird about the ocean. I would first like to thank my advisor, Tobey Curtis, for designing this project with me, welcoming me into a fantastic community of shark scientists, and always being willing to help. I would also like to thank my advisor, Paul Bologna, for the help and guidance throughout the past two years. I would like to thank my committee members, Matthew Schuler and Kyle Newton, for their expertise along the way, as well as Stephen Kajiura, Danlin Yu, and CJ Knoble for their help. I owe a huge thanks to Kevin Friedland, whose research was the steppingstone for this project and made this project possible. I would also like to acknowledge the entire team at SOFO Sharks and specifically captains Greg Metzger and Walt Zublionis for assistance with field work. Lastly, I would like to acknowledge my sources of funding for this project, the Montclair State University Wehner Student Research Scholarship and the Manasquan River Marlin and Tuna Club George Burlew Scholarship, as well as my position as a Graduate Assistant at MSU for the past year and half.

Authorization statement:

This research was formally deemed “not within the purview of IACUC review” by Montclair State University’s Institutional Animal Care and Use Committee (IACUC).

## TABLE OF CONTENTS

<b>CONTENT</b>	<b>PAGE</b>
ABSTRACT	1
SIGNATURE PAGE	3
TITLE PAGE	4
ACKNOWLEDGEMENTS	5
LIST OF FIGURES	7
LIST OF TABLES	7
CHAPTER 1 ASSESSING POTENTIAL PHYSIOLOGICAL SENSITIVITY TO ELECTRIC FIELDS VIA AMPULLAE OF LORENZINI	8
INTRODUCTION	8
MATERIALS AND METHODS	14
RESULTS	17
DISCUSSION	22
CONCLUSIONS	26
CHAPTER 2 ASSESSING SPATIAL EXPOSURE TO OFFSHORE WIND CABLES VIA GIS	28
INTRODUCTION	28
MATERIALS AND METHODS	32
RESULTS	37
DISCUSSION	45
CONCLUSIONS	48
SUMMARY (Chapters 1 and 2)	51
REFERENCES	54

## LIST OF FIGURES

<b>Figure</b>	<b>Title</b>	<b>Page</b>
1	<i>Mustelus canis</i> dorsal AOL pore arrangement.	18
2	<i>Mustelus canis</i> ventral AOL pore arrangement.	18
3	Comparison of <i>M. canis</i> size (TL) versus the total pore abundance based on sex.	20
4	<i>Leucoraja ocellata</i> ventral AOL pore agglomeration around the mouth (A) and wing (B).	21
5	Linear regression showing disc width versus pore count across juvenile and adult <i>L. ocellata</i> .	22
6	BOEM map of all current OWF lease areas off of the Atlantic coast of the U. S.	34
7	Average fall <i>M. canis</i> biomass distribution across years 2015-2019 with OWF transmission cable routes and lease areas.	38
8	Average spring <i>L. ocellata</i> biomass distribution across years 2015-2019 with OWF transmission cables routes and lease areas	39
9	Average fall <i>L. ocellata</i> biomass distribution across years 2015-2019 with OWF transmission cables routes and lease areas	40
10	Overlap of fall <i>M. canis</i> biomass with each of the 13 OWF projects.	43
11	Overlap of spring and fall <i>L. ocellata</i> biomass with each of the 13 OWF projects.	43
12	The spectrum of vulnerability to offshore wind EMFs based on the combination of physiological sensitivity and spatial exposure.	52

## LIST OF TABLES

<b>Table</b>	<b>Title</b>	<b>Page</b>
1	Measurements, head morphometrics and pore counts of adult female <i>M. canis</i> (n=4).	19
2	Measurements, head morphometrics and pore counts of juvenile male (n=3) and juvenile female (n=3) <i>M. canis</i> .	19
3	Measurements, head morphometrics and pore counts of adult male (n=1), juvenile male (n=2) and juvenile female (n=1) <i>L. ocellata</i> .	21
4	Atlantic OWFs' cable route footprints that intersect with fall <i>M. canis</i> biomass across 2015-2019	41
5	Atlantic OWFs' cable route footprint that intersects with <i>L. ocellata</i> biomass (spring and fall) across 2015-2019	41
6	Total proportions of seasonal species biomass in contact with OWF cable routes and lease areas	44



## CHAPTER ONE

### ASSESSING POTENTIAL PHYSIOLOGICAL SENSITIVITY TO ELECTRIC FIELDS VIA AMPULLAE OF LORENZINI

#### INTRODUCTION

The shift from fossil fuel-based energy to renewable energy is crucial in the marine environment to combat ocean warming and acidification, but also to meet the demands of climate change initiatives and plans of many countries. The U.S. Department of Energy's "Strategic Contributions Toward 30 Gigawatts and Beyond" aims to deploy 30 GW of offshore wind energy by 2030 and 110 GW by 2050, and the European Union aims to deploy 340 GW by 2050 (Hermans et al. 2024). By 2016, the Bureau of Ocean Energy Management (BOEM) had leased approximately 1.7 million acres of offshore wind production area in the Atlantic Ocean and developers began permitting 18 lease areas to provide just under 15,000 MW of potential electrical capacity (Musial et al. 2016).

Offshore wind turbines are connected to the onshore grid by high voltage transmission cables running underneath the seafloor. The transmission cables emit electromagnetic fields (EMFs) that are within the range of field intensities many migratory fish and marine organisms are capable of detecting (Gill et al. 2012, Hutchison et al. 2020). These subsea cables include inter-array cables between turbines, export cables transmitting electricity to shore, and interconnector cables that enable power exchange between countries (Boon et al. 2018). The EMF radiates away from the cable, which can either be alternating current (AC) or direct current (DC). Alternating current cables create a fluctuating electric field, whereas DC cables produce a static, unidirectional field (Lauria et al. 2016). Direct current cables are generally more efficient for long transmission distances because they have lower transmission losses and are therefore used for offshore wind farms (OWFs) further offshore, but AC cables are the more economic

option for transmission distances shorter than 130km (Zhang et al. 2014, Lauria et al. 2016). However, the lower cost of AC cables overall has made them the common cable type for offshore wind farms (OWFs) up until recent years even for distances up to 360km (Lauria et al. 2016). As turbines generate electricity, the electric currents running through the cables travel into both the surrounding water and substrate. Due to the higher conductivity of water, the intensity of the induced electric field is five times greater in the seawater than it is in the sand (Gill et al. 2012).

Many marine taxa are capable of magneto-sensitivity or electro-sensitivity, but only one group, the elasmobranchs (sharks, skates, and rays), are known to exhibit both (Gill et al. 2009, Gill et al. 2012, Tricas 2012, Anderson et al. 2017). Geomagnetic stimuli from the earth's magnetic field are used for navigational cues and bioelectric stimuli emitted by all species via ion exchange and respiration are used for tracking prey. Thus, anthropogenically-induced EMFs may potentially elicit both navigational and foraging responses in elasmobranchs (Bedore and Kajiura 2013, Newton et al. 2024). The benthic habits of many elasmobranch species place them near the expanding network of subsea offshore wind cables (Hermans et al. 2024). The elasmobranch subclass of Chondrichthyes has especially high electro-sensitivity compared to other marine animals because of their unique sensory structures called ampullae of Lorenzini (AOL). This sensory system allows elasmobranchs to detect potential prey and predators by encoding the amplitude and frequency of electric fields (Haueisen and Reis 2023). The level of detection or sensitivity will vary by species due to the number and arrangement of pores and the length of subdermal canals connecting pore to ampulla, which correspond to different morphologies and prey types (Kalmijn 1971, Newton et al. 2019).

Maps of the AOL, also known as pore maps, illustrate the location and density of ampullary pores visible on the dorsal and ventral sides of elasmobranchs' head and snout. As the animal grows, the canals leading from dermal pore to subdermal ampulla lengthen and the longer the canals get, the higher the animal's sensitivity becomes (Newton et al. 2019). However, recent data suggest that increasing body size comes with a tradeoff between increased sensitivity and decreased resolution, with the spatial resolution of electric stimuli decreasing throughout ontogeny (Newton et al. 2019, Crawford et al. 2024). Crawford et al. (2024) demonstrated that adult sandbar sharks had lower response thresholds to electric fields than juveniles. Essentially, the field of detection increases, but the resolution of small prey items within that field becomes coarser. It is currently understood that because they do not grow new pores, as chondrichthyans grow and age, electroreceptive resolution weakens, receptor sensitivity heightens, and their overall sensory field increases (Newton et al. 2019). It is currently believed that the number of pores is conserved with ontogeny, however a recent study found higher pore abundances in adult daggernose sharks (*Isogomphodon oxyrinchus*) as compared to juveniles (Haueisen and Reis 2023). If this is confirmed for other species, it may uncover intraspecific differences caused by changes in habitat or feeding strategy throughout ontogeny.

Electro-sensory pore distribution has been well analyzed for hammerhead sharks (family Sphyrnidae) and pore maps have been created for many other species including the sandbar shark (*Carcharhinus plumbeus*), Brazilian sharpnose shark (*Rhizoprionodon lalandii*), blue shark (*Prionace glauca*), Oman shark (*Lago omanensis*), wobbegong shark (Orectolobidae), and daggernose shark (*Isogomphodon oxyrinchus*) (Fishelson and Baranes 1998, Kajiura 2001, Poscai 2016, Newton et al. 2019, Haueisen and Reis 2023). Literature on the electro-sensitivity

of skates is more limited, but generally, more pores indicate higher sensitivity across all elasmobranch species (Kalmijn 1971, Newton et al. 2019).

Physiological and behavioral studies of elasmobranchs have demonstrated sensitivity to a wide range of electric fields as low as 5-20 nV cm<sup>-1</sup> (Kalmijn 1982) and to both direct and alternating currents (Kimber et al. 2011). While empirical studies are still limited, there is a range of potential effects from EMFs that have been suggested across the literature. Effects include disturbance of the reproductive cycle via embryonic development and mating, behavioral changes such as attraction, avoidance, or increase or decrease in activity, and impacts to migratory behavior (Hermans et al. 2024, Newton et al. 2024). Weak bio-electric fields are emitted by all prey as they respire due to the sinusoidal ventilation mechanism and ion exchange across the gills (Bedore and Kajiura 2013) and elasmobranchs use this to their advantage in foraging (Haine et al. 2001). Kimber et al. (2011) demonstrated that the small spotted catshark (*Scyliorhinus canicula*) was unable to differentiate between natural electric stimuli and artificial DC electric stimuli. Kalmijn (1982) found that both dogfish (Squalidae) and blue sharks (*Prionace glauca*) exhibited feeding responses to AC dipole electric fields implemented at sea to mimic prey. These findings suggest a critical issue for elasmobranchs with the increase of anthropogenic electric fields in the ocean. Electromagnetic field-induced behavioral changes were seen in the scalloped hammerhead shark (*Sphyrna lewini*), which demonstrated dramatic changes in swimming behavior and repeatedly bit electrodes (Kajiura and Fitzgerald 2009).

Being that magneto-sensitivity is used for long-distance migration, added anthropogenic electromagnetic fields may impact not only foraging capabilities but also migration capabilities via a potential discrepancy between Earth's geomagnetic fields and the constant, weak magnetic field from EMF-DC (Hermans et al. 2024, Newton et al. 2024). Newton et al. (2024)

demonstrated that skates (Family Rajidae) exhibited both increased and decreased activity levels when exposed to artificial AC and DC EMFs and reactions were species-specific. Big skates (*Raja binoculata*) exposed to EMFs showed increased activity and substantial changes in spatial use, while longnose skates (*Caliraja rhina*) were less active and showed different responses to different magnetic stimuli (Newton et al. 2024). It has been hypothesized that EMF-AC stimuli might be attractive to skates because the induced electric field may appear similar to the fluctuating bioelectric field emitted by respiring prey (Bedore et al. 2013, Newton et al. 2024). However, Newton et al. (2024) found that, depending on its intensity, EMF-AC may overstimulate the sensory system of skates. Big skates reduced their velocity when encountering an EMF-DC, potentially to avoid disorientation (Newton et al. 2024). Additionally, the little skate (*Leucoraja erinacea*) exhibited a prominent increase in foraging behavior when exposed to artificial EMF-DC (Hutchison et al. 2020). Behavioral responses like attraction or avoidance to EMFs could lead to changes in habitat use, predator-prey relations, and economically impact fisheries of impacted elasmobranchs (Gill et al. 2009). Understanding the biology and physiology of elasmobranchs' electro-sensory system is a crucial area of research given that the addition of anthropogenic electromagnetic stimuli may potentially impact mating, foraging, and migration (Newton et al. 2019).

The winter skate (*Leucoraja ocellata*) is a benthic elasmobranch, meaning they spend majority of their time at or near the ocean floor. Notably, skates display major shifts in diet over ontogeny (Skjaeraasen and Bergstad 2000, Szczepanski 2013). As juveniles, skates of Delaware and Narragansett Bays, as well as the North Sea, showed a preference for polychaetes, amphipods, and benthic crustaceans, but shifted to larger shrimp, squat lobster, small fish, and some gastropods and cephalopods as they matured (Skjaeraasen and Bergstad 2000, Szczepanski

2013). The smooth dogfish (*Mustelus canis*) is a bottom-oriented, demersal shark that feeds mainly on bottom-dwelling decapod crustaceans, squid, and small fish (Montemarano et al. 2016). Diet shifts over ontogeny as discussed in the rajids are also apparent in the *Mustelus* genus, with crustaceans dominating the diets of juvenile sharks, but teleosts and cephalopods dominating as sharks increase in size (Saidi et al. 2009). A heightened electro-sensory system via more AOL pores in adults may facilitate these diet changes. Benthic lifestyle and a preference for benthic prey have also been correlated to higher numbers and densities of pores (Kempster et al. 2012, Newton et al. 2019).

The purpose of this chapter was to investigate the morphology of the AOL sensory system of *M. canis* and *L. ocellata* in order to better understand their potential susceptibility to effects from offshore wind EMFs. A high pore count in either species relative to each other or to existing literature could indicate high resolution of EMF-AC, EMF-DC, or both. The goal was to assign both study species to appropriate sensitivity categories as an indicator of their vulnerability to EMFs from offshore wind development. The potential effects of EMFs on elasmobranchs are dependent upon the level of exposure and sensitivity of individual species. If species exhibit high exposure and are highly sensitive to EMFs, they are likely to show substantial behavioral or other impacts related to the location of offshore wind generation fields and transmission cables, while species showing low exposure and sensitivity are likely to be less impacted. However, for species that exhibit only one potential interacting stressor, either high exposure or high sensitivity, the outcomes of offshore wind electrical generation are more uncertain. Designation of both species to these categories may direct future research on their behavioral responses to EMFs and serves as a template for other elasmobranch species.

## MATERIALS AND METHODS

All *M. canis* specimens were caught incidentally by the South Fork (SOFO) Natural History Museum Shark Research and Education Program as part of an ongoing research project in collaboration with Stony Brook University targeting other coastal sharks. All specimens were caught off the southern coast of Long Island between Long Beach and Southampton, NY (40.5895°N, -73.6665°W to 40.88428°N, -72.38953°W). All *L. ocellata* specimens were donated by Dr. Laura Ekstrom at Wheaton College and were caught by trawl off the coast of Rhode Island. All specimens were received frozen. To account for possible ontogenetic change, pore maps of both juvenile and adult *M. canis* and *L. ocellata* age classes were evaluated.

### ***Mustelus canis* Pore Evaluation**

*Mustelus canis* pre-caudal length (PCL), fork length (FL), total length (TL), girth (G), clasper length (CL), and head morphometrics were measured to the nearest centimeter. The head morphometrics chosen followed Kajiuura (2001) and included head width (HW), head length (HL), mouth-to-snout distance (MS), mouth width (MW), internarial distance (IN), and pre-orbital length (POL). Head length was measured from the first gill to the tip of the snout. Clasper length was measured “out”, meaning from the base of the pelvic fin to the tip of the clasper. After all measurements were taken and with the specimen still frozen, the head was removed from the body at the last gill and the body was discarded. For juvenile specimens, the head was then cut in half laterally along the midline to separate dorsal and ventral surfaces. The cut followed the snout angle as closely as possible. One at a time, the dorsal and ventral halves of the head were laid on a light table and backlit to illuminate the pores. For adult specimens, the head was too large for any light to shine through the pores when placed on the light table, so the skin

was removed and backlit. The skin was removed in two pieces (dorsal and ventral) to allow for the evaluation of pores from these larger individuals. The specimen was dabbed dry to reduce reflection in the image. Pins were placed in the dissecting mat at the tip of the snout and at each eye or naris and were used as markers in the images so that each image in the series could be lined up by matching the pins to eliminate recounting of pores.

A series of photos were taken of both dorsal and ventral surfaces of each specimen with an iPhone Xs Max. The series was kept the same for each specimen and included the following photos: one from above of entire head with scale bar, one zoomed in on the top of the head from behind the eyes to the end of the head, one zoomed in on the top of the head from in front of the eyes to the tip of the snout, and one zoomed in on the left and right sides under the eyes.

Individuals for both species were identified using the following scheme: species (winter skate or dogfish (W/D)), development stage (adult or juvenile (A/J)), sex (M/F), and sample number.

Next, photos were uploaded into ImageJ software to analyze and count pores. All images were changed to 16-bit (black and white), contrast was increased, and sharpness was adjusted as necessary. The “multi-point” tool in ImageJ was used to leave a dot on each pore counted, which eliminated duplication and re-counting. The multi-point tool summarized all points added to the images and the total was recorded at the end. This was repeated to ensure that no pores were missed. Pores were counted this way on each photo from the series, then all photos with their pore markings were viewed together in one screen and cropped using the pin markers if needed, to create one seamless image of the specimen. Then, the pore counts from each of the photos (left, right, snout, whole) could be added together to give the total pore count for the ventral surface of the specimen. This process was then repeated with images of the dorsal side of the specimen. Finally, the counts from ventral and dorsal surfaces were added together to give the



total pore count for that specimen. In addition to calculating the number of pores, images were used to illustrate the spatial arrangement of pores and where they may be concentrated in high density to provide heightened sensitivity close to the mouth or nares.

### ***Leucoraja ocellata* Pore Evaluation**

*Leucoraja ocellata* disc width (DW), body length (BL), tail length (TAL), total length (TL), clasper length (CL), and head morphometrics including mouth-to-snout distance (MS), mouth width (MW), internarial distance (IN), and pre-orbital length (POL) were measured to the nearest centimeter. Because of their dorso-ventrally flattened bodies, the entire specimen was laid on the light table on both its dorsal and ventral surfaces and pores were illuminated. The specimen was dabbed dry to reduce reflection in images. Pins were placed and used in the same manner as they were for *M. canis*. A series of photos were taken of both dorsal and ventral surfaces of each specimen with an iPhone Xs Max. The series was kept the same for each specimen and included the following photos: one from above of entire head with scale bar, one zoomed in on the top of the head from behind the eyes to the end of the head, one zoomed in on the top of the head from in front of the eyes to the tip of the snout, and one zoomed in on the left and right sides. The steps taken in ImageJ to count and analyze *L. ocellata* pores were exactly the same as those discussed above for *M. canis*.

### **Statistical analysis**

In order to determine the relationship between size (i.e., age) and pore count, linear regressions were run in RStudio using the “tidyverse” package. Total length (TL) was plotted against pore count for *M. canis* and disc width (DW) was plotted against pore count for *L. ocellata*.

## RESULTS

*Mustelus canis* had an average of 1512 ( $\pm$  303 SD) electrosensory pores, 708 ( $\pm$  157 SD) in the ventral region (46%) and 830 ( $\pm$  156 SD) in the dorsal region (54%). All individuals showed very similar patterns in the arrangement of pores regardless of age or sex. On the dorsal region of the head, there was a high density of pores under the front of each eye (Figure 1). On the ventral region, pores were evenly spaced out on the length of the snout and a line of pores stretched from just above the corner of the mouth down to the outermost edge of the head, almost to the first gill (Figure 2). There was a high density of pores on either side of the mouth and below each nare (Figure 2). All adults evaluated were females (Table 1) and on average, possessed fewer pores than juveniles of both sexes (Table 2). Across adults alone, longer total length (TL) generally reflected higher pore count (Table 1), but this was not the case across juveniles (Table 2). There was a great deal of variation in pore count across individuals (Figure 3), but nine of the ten individuals had a higher number of pores in the dorsal region than in the ventral region of the head (Table 1, 2).

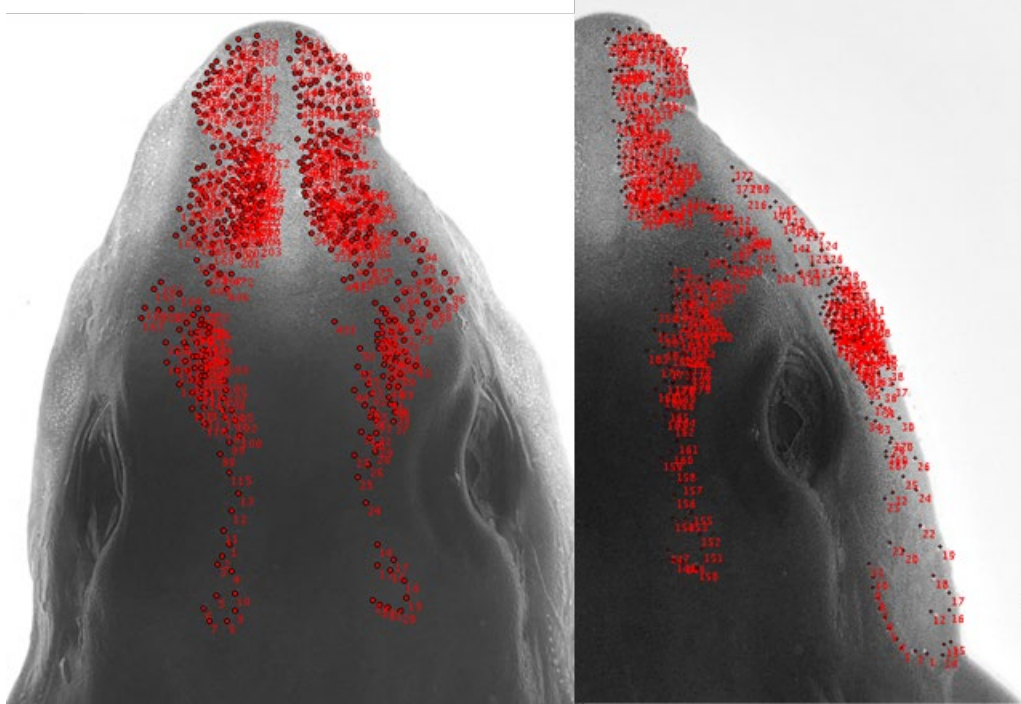


**Figure 1.** *Mustelus canis* dorsal AOL pore arrangement. Specimen shown is DJM2.

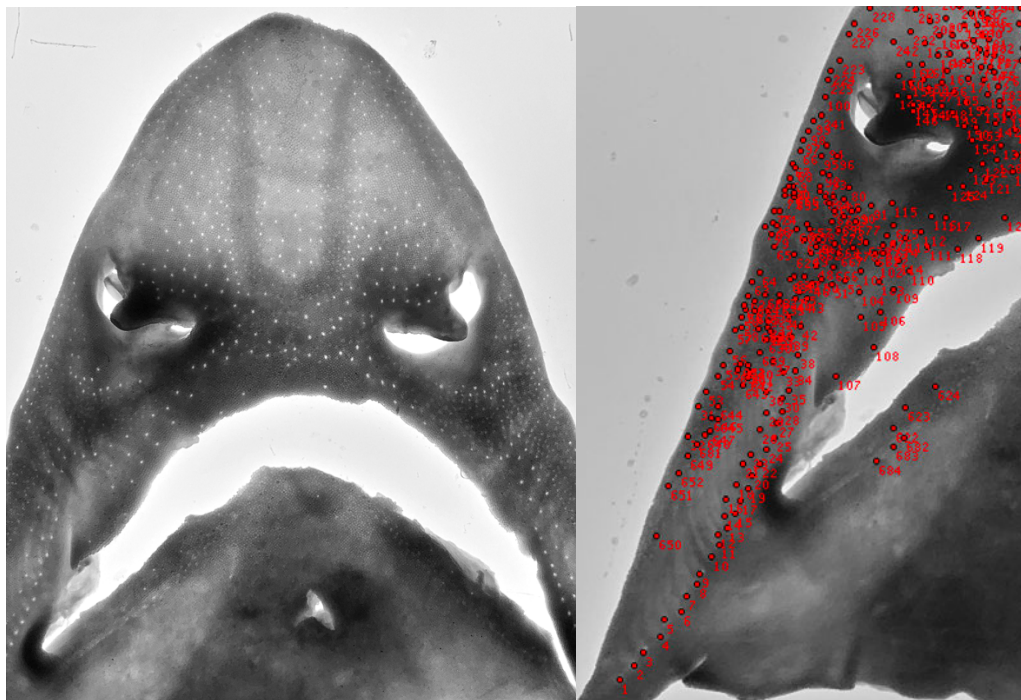


**Figure 2.** *Mustelus canis* ventral AOL pore arrangement. Specimen shown is DAF1.

**Table 1.** Measurements, head morphometrics and pore counts of adult female *M. canis* (n=4). Abbreviations: precaudal length (PCL), fork length (FL), total length (TL), girth (G), head width (HW), head length (HL), internarial distance (IN), pre-orbital length (POL), mouth-to-snout distance (MS), mouth width (MW).

	<b>DAF1</b>	<b>DAF2</b>	<b>DAF3</b>	<b>DAF4</b>
<b>PCL (cm)</b>	91.8	103	99.2	92.5
<b>FL (cm)</b>	99.2	109	107.2	106.5
<b>TL (cm)</b>	116	124.2	123.4	115
<b>G (cm)</b>	45	44.2	44.6	33
<b>HW (cm)</b>	12.8	12.8	13.2	12.3
<b>HL (cm)</b>	18.8	18.4	19	12.8
<b>IN (cm)</b>	3.5	3.4	3.5	4.1
<b>POL (cm)</b>	10.6	8	7.6	8.2
<b>MS (cm)</b>	7	7.2	6.8	6.4
<b>MW (cm)</b>	7.4	7.2	7.6	7
<b>Pore count</b>	1531 (739 ventral, 792 dorsal)	1859 (868 ventral, 991 dorsal)	1370 (607 ventral, 763 dorsal)	1289 (655 ventral, 634 dorsal)

**Table 2.** Measurements, head morphometrics and pore counts of juvenile male (n=3) and juvenile female (n=3) *M. canis*. Abbreviations: precaudal length (PCL), fork length (FL), total length (TL), girth (G), head width (HW), head length (HL), internarial distance (IN), pre-orbital length (POL), mouth-to-snout distance (MS), mouth width (MW), clasper length (CL).

	<b>DJM1</b>	<b>DJM2</b>	<b>DJM3</b>	<b>DJF1</b>	<b>DJF2</b>	<b>DJF3</b>
<b>PCL (cm)</b>	39	43.2	39	46.9	43.7	40.2
<b>FL (cm)</b>	42	47	41.2	50.4	47.4	44
<b>TL (cm)</b>	49	53.8	48.2	57.6	55.2	51
<b>G (cm)</b>	13.6	13.5	17	14	14.9	20.8
<b>HW (cm)</b>	5.2	5.6	5	5.4	5	5.2
<b>HL (cm)</b>	5.8	6	5.4	6.2	5.8	6
<b>IN (cm)</b>	2.6	2.8	2	2.4	2.2	2.4
<b>POL (cm)</b>	4	4.5	4	4.6	4.6	3.8
<b>MS (cm)</b>	3.8	4	3.6	4.1	4	3.6
<b>MW (cm)</b>	3	3.6	3.2	3.8	3.2	3.2
<b>CL (cm)</b>	1.7	1.8	1.8	-	-	-
<b>Pore count</b>	1774 (798 ventral, 976 dorsal)	1847 (839 ventral, 1008 dorsal)	1223 (482 ventral, 741 dorsal)	1924 (936 ventral, 988 dorsal)	1052 (477 ventral, 575 dorsal)	1513 (683 ventral, 830 dorsal)

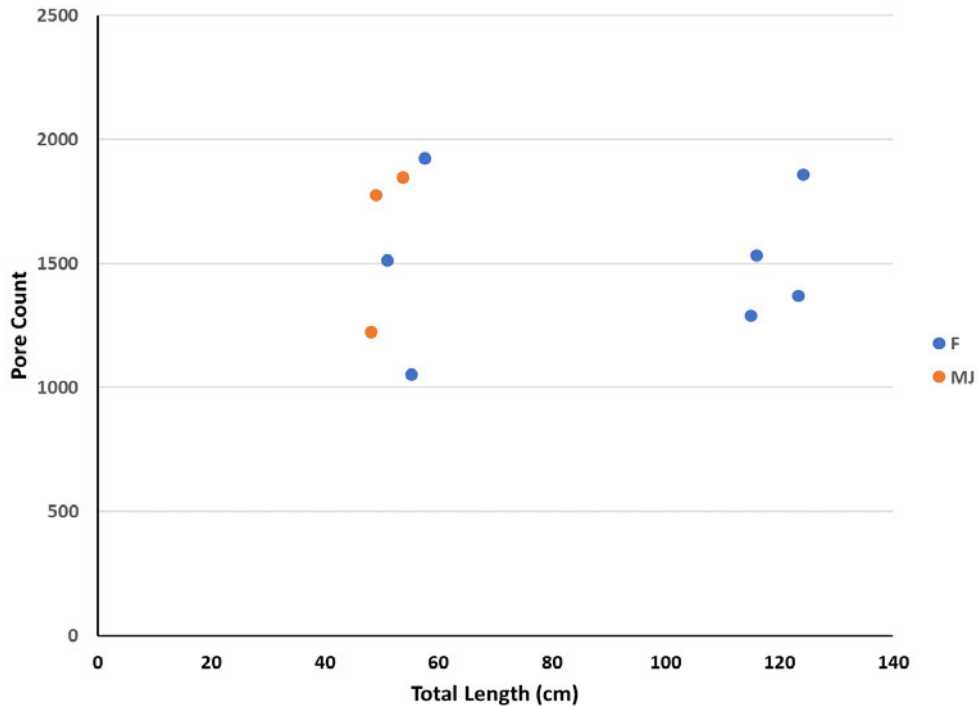


**Figure 3.** Comparison of *M. canis* size (TL) versus total pore abundance based on sex. Adult *M. canis* were all females. F = females, MJ = males (juvenile).

A linear regression was conducted to examine the potential relationship between total length and pore count. The model was not significant ( $F = 0.009$ ,  $p > 0.9$ ) and accounted for only 0.122% of the variance in pore count ( $R^2 = 0.0012$ ). An additional linear regression was conducted across adults only to examine the same relationship. While the model explained 30% of the variation in pore count ( $R^2 = 0.3$ ) and found a slightly positive relationship between TL and pore count across adults, it was not significant due to small sample size ( $p > 0.4$ ).

*Leucoraja ocellata* specimens had pore counts ranging from 381 to 741, with an average of 476 ( $\pm 176$  SD) electrosensory pores, all in the ventral region of the head (Table 3). During the evaluation, no pores were located on the dorsal surface of any individuals. Unlike *M. canis*, *L. ocellata* exhibited substantial variation between juvenile and adult specimens. The three juvenile specimens had an average of 388 pores, while the single adult specimen had 741 pores. There was no observed variation in the pattern of AOL pore arrangement on the ventral region of

*L. ocellata*. All specimens showed the highest density of pores around the mouth (Figure 4A) and similar arrangements on each wing (Figure 4B).

**Table 3.** Measurements, head morphometrics and pore counts of adult male (n=1), juvenile male (n=2) and juvenile female (n=1) *L. ocellata*. Abbreviations: disk width (DW), body length (BL), tail length (TAL), total length (TL), clasper length (CL), mouth width (MW), mouth-to-snout distance (MS), internarial distance (IN).

	WAM1	WJM1	WJM2	WJF1
<b>DW (cm)</b>	61.2	21.6	23	27.2
<b>BL (cm)</b>	38.4	16	19.8	25.6
<b>TAL (cm)</b>	37.2	20.4	16.8	24.2
<b>TL (cm)</b>	75.6	36.4	36.6	49.8
<b>CL (cm)</b>	15	2.2	1.2	-
<b>MW (cm)</b>	9.2	5.6	2.2	2.6
<b>MS (cm)</b>	12.8	7	6.8	8.2
<b>IN (cm)</b>	8.6	5	2.4	3
<b>Pore count</b>	741	398	384	381

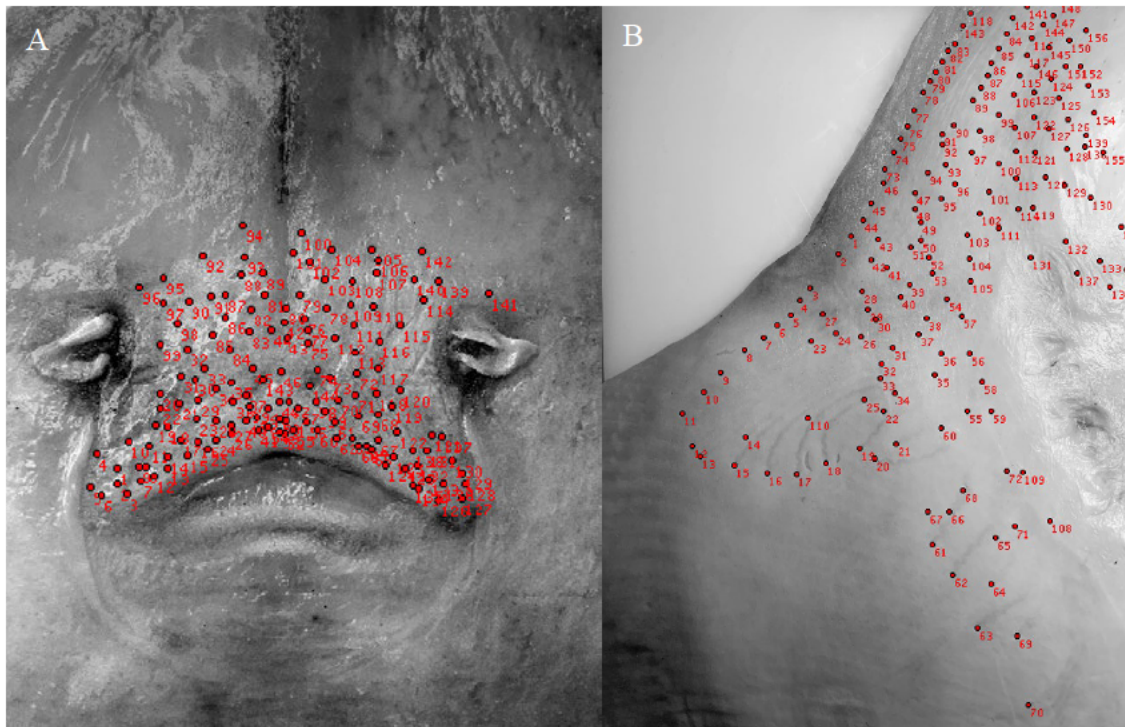


**Figure 4.** *Leucoraja ocellata* ventral AOL pore agglomeration around the mouth (A) and wing (B). Specimen shown is WJM2.

A linear regression was conducted to examine the potential relationship between disc width and pore count (Figure 5). The model found a significant positive linear relationship between disc width and pore count ( $F = 74.3$ ,  $p = 0.013$ ,  $df = 3$ ), which accounted for 97.4% of the variance in pore count ( $R^2 = 0.974$ ). However, sample size was low for *L. ocellata*, limiting a more robust statistical assessment.

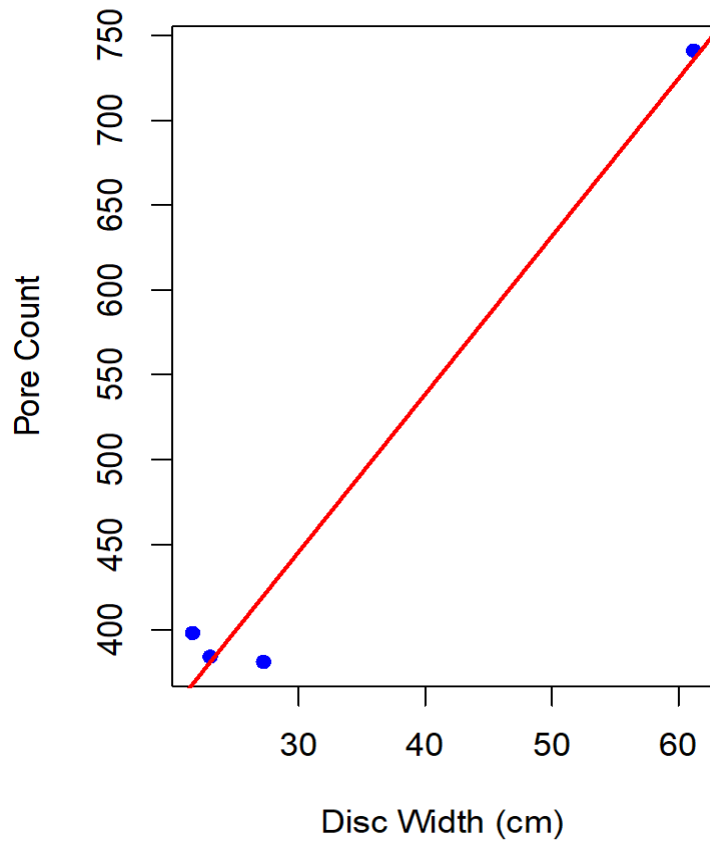


**Figure 5.** Linear regression line showing disc width versus pore count across juvenile and adult *L. ocellata*.

## DISCUSSION

These results provide a first characterization of AOL pore counts and distributions for two common, commercially important elasmobranch species. The analyses will help assess the

potential sensitivity of these species to EMFs associated with offshore wind. The average number of electroreceptor pores in *M. canis* (1512) was higher than that of *L. ocellata* (476) and falls in the mid-to-upper region of the entire range of pores in Carcharhiniformes. This suggests that *M. canis* has a relatively high-resolution electrosensory system, as a greater abundance and density of pores generally reflects higher resolution of electrical stimuli (Newton et al. 2019). The average pore count for adult *M. canis* (1512) falls just above the median of the overall range (237 to 3067) of pores in other Carcharhiniformes that have been analyzed (Kempster et al. 2012). Sphyrnid sharks are known to have some of the highest pore counts (2028 to 3067) due to the elongated cephalofoil that expands the subdermal canals (Kajiura 2001). Additionally, the daggernose shark (*Carcharhinus oxyrinchus*), with 3943 pores, has an elongated snout (Hauelsen and Reis 2023). Thus, the small size of the head and snout of *M. canis* aligns with its pore count.

It is important to note here that for the purpose of illustrating overall vulnerability to effects from offshore wind EMFs, the word sensitivity is used to infer resolution of electric stimuli. Sensitivity is more associated with the number of sub-dermal receptor cells and the length of ampullary canals rather than pore counts (Raschi 1986, Newton et al. 2019). Resolution stems from the abundance of AOL pores, whereas sensitivity stems from longer canals and larger ampulla, which were not analyzed in this study. Ideally, diffusible iodine-based contrast-enhanced computed tomography (diceCT) would be used to image the sub-dermal ampullae network of both species in order to obtain a true measure of electro-sensitivity. DiceCT is used for imaging animal soft tissues like the brain, but it has been used to describe the nervous and olfactory systems in an elasmobranch and teleost (Camilieri-Ash et al. 2020).



It is not unusual to have variation in pore count across a single species, but it is understood that that number stays consistent throughout the animal's life (Kajiura 2001, Kempster et al. 2012, Newton et al. 2019). There was a great deal of variation across *M. canis* individuals, which was not unexpected based on recent pore counts of the daggernose shark by Haueisen and Reis (2023), who found ontogenetic variation in pore abundance, a first in elasmobranch electrosensory research. Haueisen and Reis (2023) found significantly higher pore abundances in adult daggernose sharks compared to juveniles, but no significant variation among sexes. The variation in *M. canis* pore counts across individuals in the current study was large (Figure 3), however there was no consistent pattern corresponding to age classes, so ontogenetic variation in *M. canis* cannot be concluded. However, for *L. ocellate* there was a positive relationship between pore count and size of individual (Figure 5), similar to the findings of Haueisen and Reis (2023), but the small sample size of this study limits the ability to robustly characterize these relationships.

While juvenile *M. canis* exhibited higher pore counts on average than adults, this does not indicate that pores are lost with age. The increase in number of pores between growth stages illustrated by Haueisen and Reis (2023) in the daggernose shark may be explained by intraspecifically distinct habitats or feeding techniques in different life stages that reflect a need for higher resolution. For example, life stages spent living and feeding in turbid estuary waters may facilitate a need for a higher resolution electro-sensory system as adults (Haueisen and Reis 2023). As adult *M. canis* have been predicted in higher abundance in estuaries and inshore coastal waters that are lower in salinity and higher in turbidity due to sediments, these intraspecific differences are possible. There was a slightly positive correlation between TL and pore count found across the four adult female specimens, but it was not significant. Additionally,

there appears to be no difference in pore counts between the three juvenile females and four adult females, as well as in the distribution of pore counts between male and female juveniles (Figure 3). Further research with a larger sample size across more age and growth classes is needed to determine if ontogenetic differences exist or if differences exist between sexes.

A higher density of pores on the ventral surface as shown in *L. ocellata*, indicates preference for benthic prey. The even distribution in *M. canis* indicates that they feed on both benthic and pelagic prey, however diet analysis for *M. canis* from the region where samples were collected documents very high percentages of benthic prey in all individuals (Montemarano et al. 2016). A high number of pores on both the ventral and dorsal regions is advantageous for detecting prey both above and below them in the water column (Kajiura 2001). This is necessary for *Mustelus* sharks, as they are known to shift from one diet source to another as they grow (Saidi et al. 2009). The area underneath the small eyes of *M. canis* exhibited a high density of pores. In regions with reduced visual cues, *M. canis* often relies upon chemoreception to track food resources at a distance, but may rely upon bioelectric fields emitted by prey to strike (Kalmijn 1982), indicating that EMF presence may impact feeding behavior.

The lower abundance of pores exhibited by *L. ocellata* indicates a lower resolution electrosensory system. However, the dorsoventrally flattened morphology of the Rajidae family in general may impact the length of ampullary canals, therefore creating a heightened sensitivity (Raschi and Adams 1988, Newton et al. 2019), but this could only be determined through use of diceCT. There was no evidence of variation in the pattern of pore distribution between sexes or among different sizes *L. ocellata* specimens. This is consistent with the limited literature on AOL counts of other members of the Rajidae family found by Raschi and Adams (1988) and Zhang et al. (2018). The ventral pore arrangement of *L. ocellata* indicates the important role that

electroreception plays in the species' feeding. The position of the mouth on dorsoventrally flattened rajids seemingly eliminates the use of vision during feeding and the concentration of AOL pores around the mouth likely compensates for this by creating an increased sensitivity for prey capture. Contradictory to pore arrangements of the thorny skate (*Amblyraja radiata*) by Raschi and Adams (1988), there were no pores visible on the dorsal region of any *L. ocellata* specimens, juvenile or adult. However, this could be due to photo resolution and there may be pores on the dorsal surface that could not be seen with the methods used in this study.

Acknowledging the small sample size, there was a positive linear relationship between disc width and pore count in *L. ocellata* (Figure 5). This indicates that an increase in electrosensory resolution may potentially facilitate the diet shifts to faster prey items exhibited by adult rajids. Inability to obtain a larger sample size for *L. ocellata* constrains the results. The reliability of the regression analysis on the relationship between *L. ocellata* disc width and pore count is very weak due to only having a single adult specimen. Additional adult specimens with a different pore count could substantially change the regression and would have improved the strength of this test. Regardless of whether increased pore abundance across ontogeny is confirmed, electroreceptive resolution changes throughout an elasmobranchs' life as resolution decreases with age, while sensitivity increases. Assuming this is true, juveniles may be more susceptible to false strikes in foraging due to their reliance on high resolution, but adults may be more likely to miss prey items all together because their resolution is much coarser.

## CONCLUSIONS

The results presented here are considered to be preliminary data for both species because previous pore counts do not exist. The goal of this research was to provide a template for continued AOL research on the two species. Based on AOL pore counts, *M. canis* exhibits a

higher resolution electrosensory system relative to its size, with pore densities and arrangement well-developed for feeding on both benthic and pelagic prey. The electrosensory system of *M. canis* exhibits a high degree of variation at the individual level, but not across ontogeny. Relative to *M. canis*, the electrosensory system of *L. ocellata* seems to have a much lower resolution, but limited literature and pore counts for other rajids makes it difficult to compare on a relative scale. It is also possible that while being low resolution, the electrosensory system of *L. ocellata* is highly sensitive due to head morphology (Newton et al. 2019). Sample size also restricts the ability to extrapolate the results of the AOL pore counts for *L. ocellata*. Nonetheless, the arrangement of pores on the ventral surface illustrates its reliance on benthic prey. The consistent higher abundance of AOL pores on the dorsal region of *M. canis* and the higher abundance of AOL pores in adult *L. ocellata* highlight the ontogenetic diet shifts exhibited by both species.

## **CHAPTER TWO**

# **ASSESSING SPATIAL EXPOSURE TO OFFSHORE WIND ELECTROMAGNETIC FIELDS VIA GEOGRAPHIC INFORMATION SYSTEMS (GIS)**

## **INTRODUCTION**

The northeast sparked the first offshore wind development for the U.S. for good reason. Coastal regions throughout the world have especially high energy demands because of high populations centers. The northeastern U.S. is a special case of this, as almost 20 percent of the entire country's population lives in two percent of its land (Seelye and Salem 2014). Offshore wind farm (OWF) development sites are chosen based on multiple factors including viewshed analysis, avoidance of military areas, and availability of wind resources, but planning does not automatically exclude fishing grounds with competing use (Methratta et al. 2020). Rather, according to the Energy Policy Act of 2005, site determination must include "consideration" of fishing activities (Methratta et al. 2020). This consideration is a responsibility of the National Marine Fisheries Service (NMFS) through determining essential fish habitat (EFH), which is then provided to the Bureau of Ocean Energy Management (BOEM) as part of a technical assessment. The process of EFH designation includes a statement of all the fish and invertebrate species to which the proposed area is especially important during any life stage, followed by a detailed description of how each species uses the habitat. There is also designation of habitat areas of particular concern (HAPCs), which are subsets of EFH that are extremely important to a fish or invertebrate species or are vulnerable to degradation (Methratta et al. 2020, Chaji and Werner 2023). Even if HAPCs are identified during the evaluation process, they do not require any particular protection or restriction from OWF development (Methratta et al. 2020). BOEM has all oversight responsibility of offshore wind planning in federal waters.

The U.S. has very ambitious goals for offshore wind energy production in the coming decades and it is extremely important that we assess the impacts they may have to marine life. Offshore wind energy in the U.S. is currently about a \$39 billion industry (Musial et al. 2023), while commercial fish landings in the U.S. totaled \$5.5 billion in 2019 and \$4.8 billion in 2020 alone (Chaji and Werner 2023, National Marine Fisheries Service 2020). Currently designated lease areas for OWFs cover 2.3 million acres of the U.S. northeastern continental shelf and will impact 14 different NOAA fisheries surveys (Methratta et al. 2023). Development of offshore wind in the northeastern shelf will overlap with numerous fisheries that contribute important economic, recreational, and cultural resources (Methratta et al. 2020). Offshore turbines are connected to onshore stations by high voltage transmission cables running underneath the seabed, some at a minimum burial depth of two meters (NMFS 2020). These cables emit electromagnetic fields (EMFS) that elasmobranchs are capable of detecting via ampullae of Lorenzini (AOL) (Hutchison et al. 2021, Methratta et al. 2023). Anthropogenic changes to the marine environment have cascading effects on impacted populations and ecosystems, so it is crucial that research on the impacts of offshore wind to elasmobranchs and other electrosensitive animals keeps pace with OWF project development. Offshore wind shows promising potential for a renewable energy economy, but commercial and recreational fisheries' economic value may be impacted if not taken into careful consideration (Chaji and Werner 2023).

The winter skate (*Leucoraja ocellata*) fishery is one of the largest commercial fisheries in the northeastern United States and they are harvested for wing meat for human consumption and for lobster bait (NOAA 2023a). While *L. ocellata* has been listed as endangered by the IUCN Red List of Threatened Species based on Canadian populations (Kulka et al. 2020), this is not the case for the U.S. population (NOAA 2023a). As of the 2022 stock assessment, the U.S.

*L. ocellata* fishery is not overfished and is not subject to overfishing (NOAA 2023a). Skates are the dominant elasmobranch commercially harvested in the U.S., with landings doubling those of all shark species (Curtis and Sosebee 2015). The species composition of skate landings in both the Gulf of Maine and southern New England ports has shown shifts to complete domination by *L. ocellata* (Curtis and Sosebee 2015). In the Gulf of Maine, *L. ocellata* made up 62% of the skate landings in 2005, but 100% in 2012 (Curtis and Sosebee 2015). While the northeastern U.S. skate complex is comprised of seven species, winter and little skates are the only stocks large enough to be targeted by fisheries (Curtis and Sosebee 2015). Managing all skate species together as a stock complex makes it difficult to assess fishing impact to each individual species (Curtis and Sosebee 2015, Kulka et al. 2020). Thus, a decline in *L. ocellata* landings due to displacement from offshore wind may be masked by the multi-species catch trends. *Leucoraja ocellata*, like all other skates, is a benthic elasmobranch, meaning they spend majority of their time on or near the ocean floor. This means that they may be particularly exposed to EMFs emitted by high voltage OWF transmission cables buried underneath the sea floor (Hermans et al. 2024).

The smooth dogfish (*Mustelus canis*) is a small shark abundantly found throughout inshore waters of the western Atlantic from Massachusetts to Florida (Conrath 2000). The smooth dogfish was chosen to represent another commercially important species to northeastern U.S. fisheries, while also analyzing the difference in potential offshore wind impact between true benthic species (winter skate) and a demersal, meso-pelagic species. Smooth dogfish have historically been collected for dissections, but commercial landings began to increase in the U.S. in the 1990's, commonly used for meat for fish and chips in England (Conrath 2000, NOAA 2023b). The fishery was valued at over \$100,000 for the year 1992 (Roundtree 1996), but this

has increased in more recent years as the fishery has grown in the northeast. Landings in 2022 totaled 375 mt (> 825,000 lb.) in the Atlantic region, but this was only 17% of the year's quota (NOAA 2023b). *Mustelus canis* primarily inhabits continental shelves and shallower inshore waters up to 200m depth (Dell'Apa et al. 2018, Conrath 2000). As a demersal, bottom-feeding species, the smooth dogfish spends little time in pelagic waters and almost all its targeted prey are either crustaceans, mollusks or small fish on or near the benthos (Roundtree 1996, Montemarano et al. 2016). The smooth dogfish is highly migratory, found in the Carolinas and Chesapeake Bay during the fall and winter seasons and traveling to the mid-Atlantic and southern New England in late spring and summer (Dell'Apa et al. 2018). Thus, spatial analyses of habitat and offshore wind overlap across different seasons may give insight into what overlap patterns may look like for other highly migratory sharks.

OWFs have four possible types of direct effects on fish and fisheries: the artificial reef effect, fisheries exclusion, energy landscape effects, and fisheries displacement (Bergström et al. 2014). Long-term spatial analyses between elasmobranch species and offshore wind will give insight into all four of these effects. If either species' geographic distribution has significant overlap with offshore wind lease areas or transmission cable routes, specifically within a region of fisheries exclusion or restriction, the fishery may experience changes in catch rates or the fishery itself may shift geographically. According to Bergström et al. (2014), if a fishery is reallocated to another geographical area after OWF establishment, the new fishing area could either be more or less resilient to fishing pressure.

This chapter aims to illustrate the extent to which offshore wind development in the mid-Atlantic spatially overlaps with smooth dogfish and winter skate fisheries biomass estimates. These analyses provided a measure of exposure of both species to offshore wind development.



By combining this measure of exposure with the previous chapter about the electrosensitivity of the winter skate and smooth dogfish, we can understand the overall vulnerability of both species to potential behavioral impacts from offshore wind development.

## **MATERIALS AND METHODS**

To illustrate the overlap of offshore wind development with smooth dogfish and winter skate habitat, a measure of total area overlap between OWF transmission cables and fisheries biomass per offshore wind project was calculated. Additionally, the proportion of species biomass that falls within an area affected by offshore development in any way (transmission cables versus lease area/turbine substrate) compared to the total species biomass across the entire study area was calculated. To assess the interactions between OWF development and the distribution of the smooth dogfish and winter skate, data were obtained from a fishery-independent bottom trawl survey conducted by the NOAA Northeast Fisheries Science Center in the spring and fall of each year. The trawl survey began in 1963 for fall sampling and 1968 for spring sampling and covers areas from the coast of North Carolina to Nova Scotia (Friedland et al. 2021). Data including location, sea surface temperature, bottom water temperature, and salinity are collected, as well as the number of individuals and total weight of 169 different species encountered during surveys (Friedland et al. 2021). The study area was defined as Cape Hatteras, North Carolina to Cape Cod, Massachusetts. The timeline of 2015 through 2019 was chosen to analyze a period of rapid offshore wind development. This study area contained only 11 planned OWF lease areas as of 2015 and as of 2024 contains 19 (Figure 6). For both study species, the smooth dogfish and winter skate, years 2015 through 2019 were selected in order to capture a time period where permitting for lease areas was expanding and some projects'

construction had begun (South Fork Wind). Species distribution models (SDMs) estimating biomass were generated using the Random Forest Model and fitted onto a 0.1-degree grid by Friedland et al. (2021). This model built trees of all of the predictor variables recorded in the survey, such as water temperature and depth, in order to predict the distribution of biomass for both species of concern. The surveys provided catch per unit effort ( $\log_{10}[\text{CPUE kg tow}^{-1} + 1]$ ) of biomass and the random forest regression model was fitted on log-transformed biomass catch (kg) per tow; therefore, the model biomass units were kg/tow (Friedland et al. 2021). With two study species, two seasons, and five survey years, 20 SDMs were generated by isolating the species, season, and year (e.g. “SmoothDogfishFall2019.rast”). All 10 SDMs for each species were imported individually into *RStudio* as a raster data file (.rast) and raster calculator was used to calculate an average biomass across 2015 to 2019 for spring and fall seasons. This produced four seasonal heat maps based on surveys (spring, fall) illustrating the average biomass for the smooth dogfish and winter skate across mid-Atlantic and New England coasts. Spring *M. canis* data were omitted from the study because their distribution is very limited in the study area during these months. The three heat maps were then imported into ArcGIS Pro and QGIS as raster files to begin three separate spatial analyses. It is worth noting that, because of the expansive area covered by the trawl survey, the pixel size of the raster data in GIS was comparatively coarse, which limits the reliability of any distance or specific geographic locations in GIS analyses. Ideally, a more appropriate model would be designed for the specific needs and timeframe of this research and used to build new species distribution models. Preliminary maps were generated in ArcGIS Pro, but all final maps as well as all spatial analyses were generated and conducted in QGIS version 3.32.3-Lima on a macOS High Sierra version 10.136.

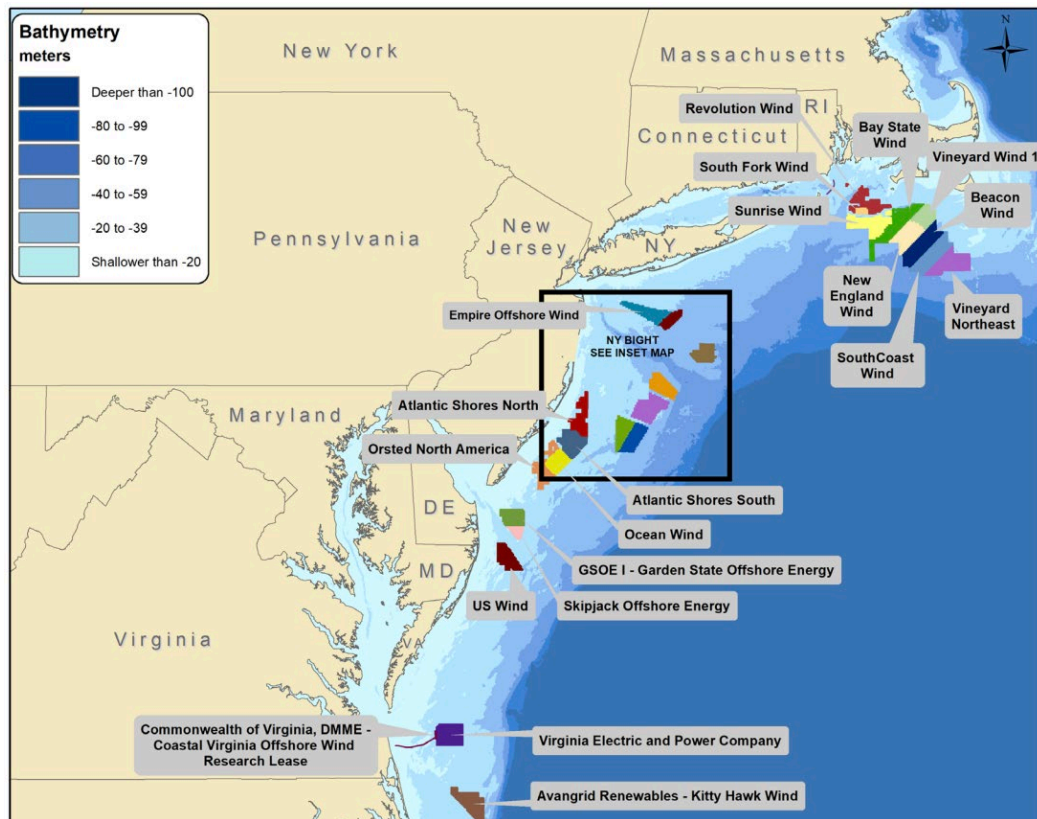


**Figure 6.** BOEM map of all current OWF lease areas off of the Atlantic coast of the U.S. URL: <https://www.boem.gov/sites/default/files/documents/renewable-energy/state-activities/Atlantic%20OCS%20Renewable%20Energy%20Lease%20Areas.pdf>

### Spatial Analysis in QGIS

Data were separated by species and season, generating three separate maps for analyses (*M. canis* fall, *L. ocellata* spring, *L. ocellata* fall). All analyses were conducted in the same manner for all species biomass maps. For illustrative purposes, I use *M. canis* fall biomass data as an example. With the raster layer shown as a heat map of *M. canis*' fall biomass distribution added to a blank QGIS project, three shapefiles from the Bureau of Ocean Energy Management (BOEM) and Northeast Ocean Data Portal were added to the map (Figure 7). These showed export cables, proposed offshore wind lease areas, and active offshore wind lease areas in

federal waters. First, to account for the fact that elasmobranchs can sense EMFs from a relatively short distance, a buffer of 50 meters was added to all export cable layers using the “Pairwise Buffer” tool. The new buffer layer was then dissolved (Vector geometry-> “Dissolve”) by project name, thus showing the single cable that corresponded to each offshore wind project. This yielded 13 separate buffers (and their transmission cables) corresponding to the 13 different OWF projects in the study area. Spatial analysis cannot be conducted between raster and vector layers, therefore each individual pixel of the raster was transformed into its own polygon using the “Raster pixel to polygon” tool. Then, the vector polygons created were classified into five classes according to biomass values inside by navigating to symbology and selecting “Graduated” symbology, “VALUE” in the value field, “Natural Breaks (Jenks)” for the mode, and clicking “Classify”. With the vector polygons broken into five distinct classes by increasing biomass, the original raster layer was reclassified to match the vector one using the “Reclassify by table” tool. Five classes were created identical to the ones in the vector layer. Next, a spatial join was done to identify all pixels that contained data from both the vectorized *M. canis* biomass layer and the cable buffer vector layer (Vector general-> “Join attributes by location”; Join to features in: “*M. canis* biomass” vector layer; Where the features: intersect; By comparing to: “dissolved buffer” vector layer; Fields to summarize: “project name”; Summaries to calculate: “count”). This counted all pixels that, for each offshore wind project, contained any fish biomass intersected by a cable or its buffer, highlighting all area of overlap between OWF cables and *M. canis* biomass. Cable buffer was chosen as the input as opposed to the cable layer itself because the buffer layer includes both the underlying cables and the 50-meter buffer around them. The new layer created by the spatial join had to then be dissolved again by project name. The final attribute table from the dissolved spatial join contained the 13 OWF cables and

the “count” of how many pixels they intersected that contained *M. canis* biomass (Table 4). The “count” extracted presence-absence data rather than fish biomass in grams. For example, the spatial join identified 22 pixels where Sunrise Wind intersected with *M. canis* biomass, 13 pixels where South Fork Wind intersected with *M. canis* biomass, and so on. Next, to calculate the actual area of overlap between *M. canis* distribution and OWF cables, the “count” for each project was multiplied by the pixel resolution of the map. To determine the resolution, it was first ensured that all layers of the project in QGIS were projected to a coordinate system that preserves distance, such as an equidistant conic projection. The North American Datum 1983 (NAD83) Equidistant Conic projection was used for all maps, which measures using latitude and longitude and therefore uses degrees as units. Each biomass pixel on the map was equal to 0.0414 degrees, or 16 km<sup>2</sup>. The spatial join provided the “count” of biomass pixels intersected by each OWF projects’ cable footprints. To calculate overlap area, the pixel count was multiplied by the area of each pixel (16km<sup>2</sup>) (Area of Overlap=Biomass Pixel Count×16km<sup>2</sup>).

As a second measure of potential offshore wind impact on both species, the proportion, or percentage, of the entire study area potentially impacted by offshore wind in any way (transmission cable EMFs, sound, structure) was analyzed. To do this, total average *M. canis* biomass across the entire study area was summed by season using the “identify features” tool in QGIS. Then, the total biomass intersected by each of the 13 OWF’s cable route or 50-meter cable buffer was summed using the same “identify features” tool, selecting each cell that was highlighted by the spatial join as overlapping with cable buffer, and recording the biomass value inside. The spatial join done previously created a new layer with each of the 13 OWF projects in a different color, making it easier to differentiate biomass totals within each individual project. The total biomass inside the spatial join layer was then divided by the total *M. canis* biomass

across the entire study area to calculate what percent of the population is subject to potential impact specifically from EMFs emitted by the high voltage transmission cables of OWFs. Next, this same approach was taken with regard to lease area, rather than cables routes. Biomass within any of the 13 designated (not planned) lease areas was summed and again divided by the total biomass for the study area. This calculated the percentage of the population subject to potential impact from OWF lease area via structure, sound, fish aggregating device (FAD) effect, etc. Lastly, biomass within lease area and biomass within cable routes were added together and again divided by the total biomass across the study area to provide a percentage of the population subject to potential impact either from OWF activity of any kind, whether from cable EMFs or physical lease area construction and operation. This process was repeated with *L. ocellata* spring and fall data.

## RESULTS

### Calculated Biomass Patterns

*Mustelus canis* and *L. ocellata* are widely distributed across the study site. Fall *M. canis* biomass patterns showed highest density in shallow, nearshore waters from the Delaware Bay to Cape Cod, Massachusetts, but there is also significant biomass offshore in Georges Bank (Figure 7). Spring *L. ocellata* biomass patterns demonstrated a broad distribution all along the study region, but higher biomass in the northern regions off the east coast of Massachusetts (Figure 8). The densest spring *L. ocellata* biomass is found in Georges Bank (Figure 8). For fall *L. ocellata* biomass patterns, the distribution is almost entirely in the northern regions off the east coast of Massachusetts, with very little biomass captured south of New Jersey (Figure 9). Both species showed very similar geographic ranges, but the seasonal shift from nearshore to offshore is

apparent in the *L. ocellata* spring and fall models, respectively (Figure 8, 9). Species distribution models for spring *M. canis* showed very low biomass in the study area, which is why they were not included.

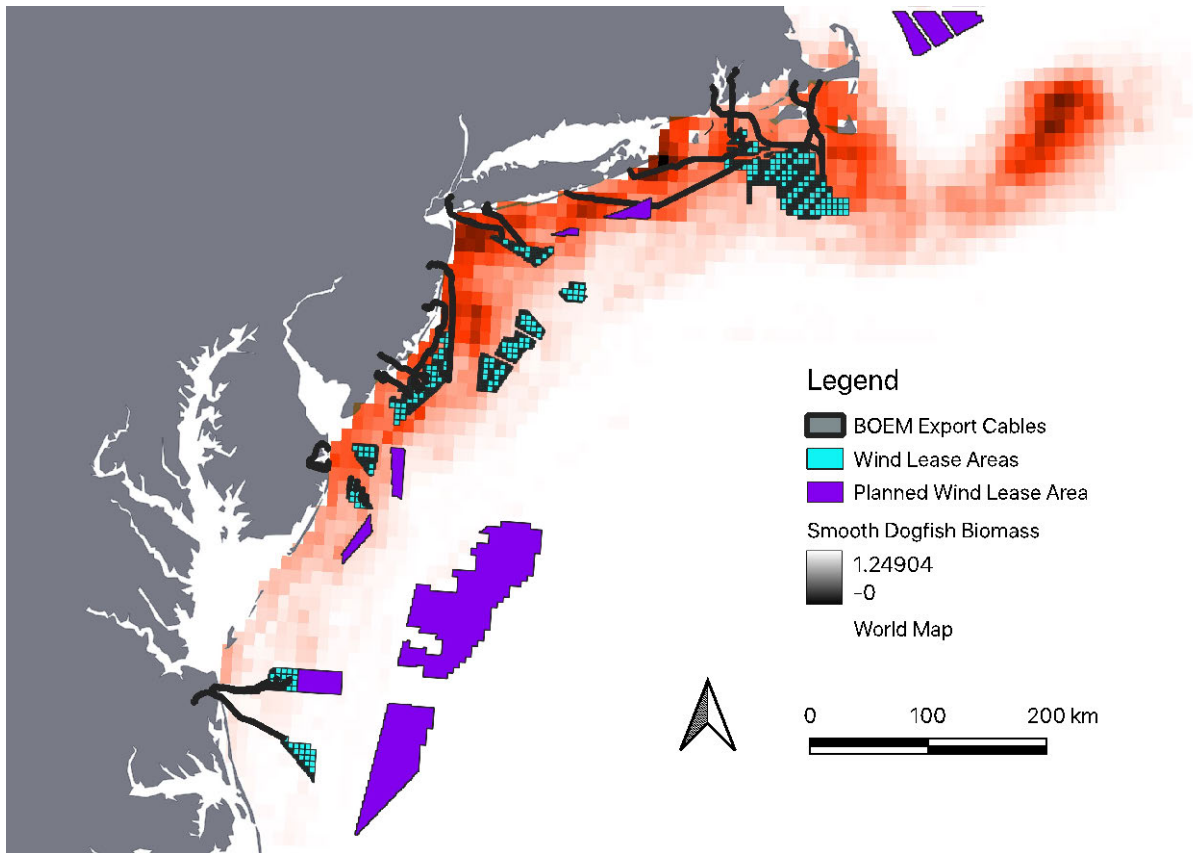


**Figure 7.** Average fall *M. canis* biomass distribution across years 2015-2019 with OWF transmission cable routes and lease areas. Wind lease areas are shown in teal/light blue, and planned lease areas are shown in purple. Red coloration represents relative smooth dogfish biomass, with darker red signifying more biomass. The color spectrum for biomass is inverted on the map legend.

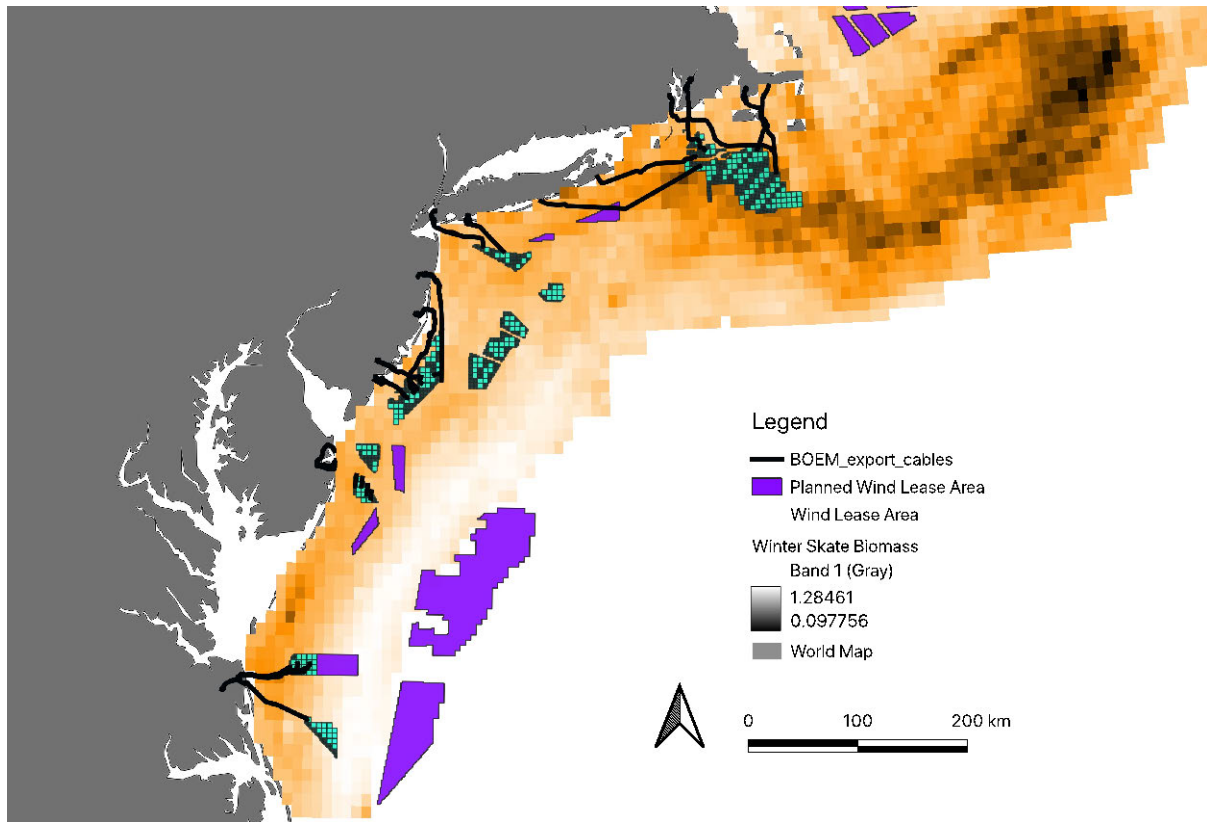


**Figure 8.** Average spring *L. ocellata* biomass distribution across years 2015-2019 with OWF transmission cables routes and lease areas. Wind lease areas are shown in teal/light blue, and planned lease areas are shown in purple. Orange coloration represents relative winter skate biomass, with darker orange signifying more biomass. The color spectrum for biomass is inverted on the map legend.



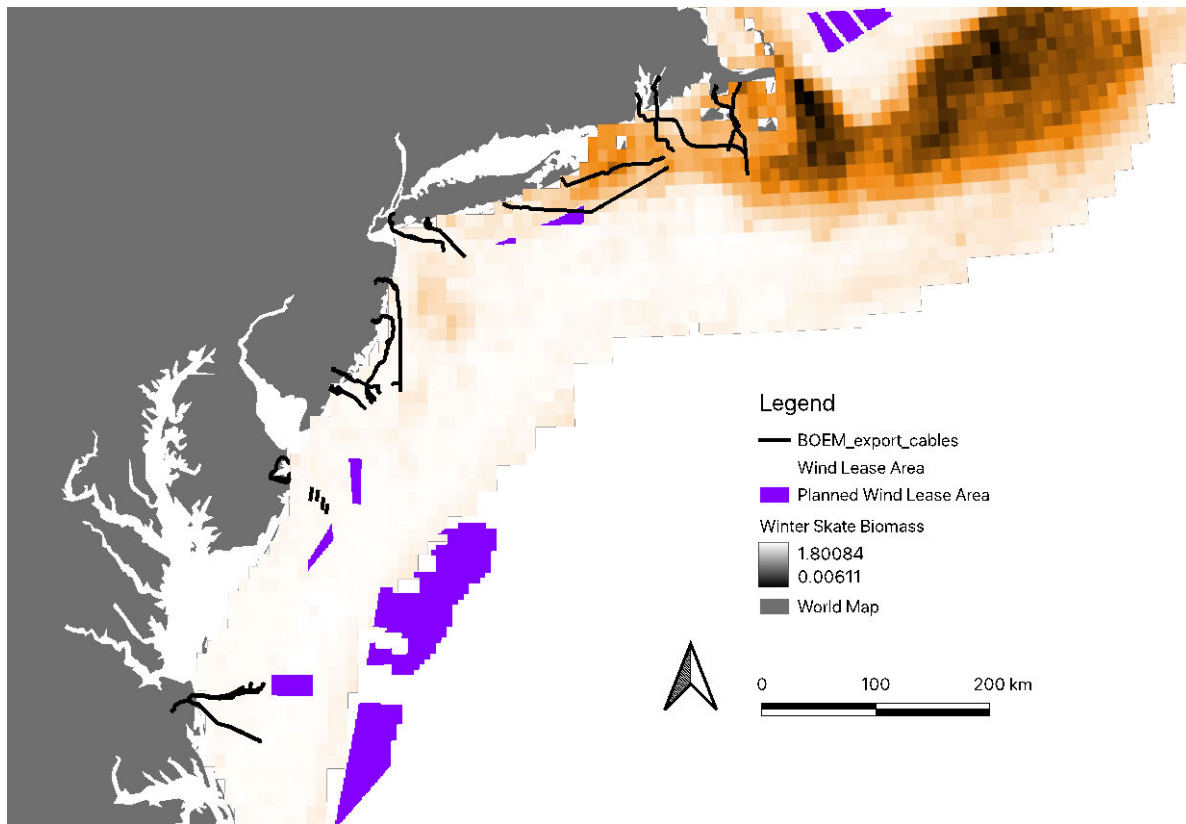


**Figure 9.** Average fall *L. ocellata* biomass distribution across years 2015-2019 with OWF transmission cables routes and lease areas. Wind lease areas are shown in teal/light blue, and planned lease areas are shown in purple. Orange coloration represents relative winter skate biomass, with darker orange signifying more biomass. The color spectrum for biomass is inverted on the map legend.

### Calculated Potential Area of Overlap

Fall *M. canis*, spring *L. ocellata*, and fall *L. ocellata*'s calculations all yielded the same 13 OWFs in only slightly different order of overlap area (Tables 4, 5). The total “count” of cells where cables intersected biomass ranged from four to 22, totaling 2,256 km<sup>2</sup> of cable route footprints intersecting fall *M. canis* and 2,240km<sup>2</sup> intersecting spring *L. ocellata* and fall *L. ocellata*. *Leucoraja ocellata* distribution shifts heavily offshore in the fall season, but the northern and southern limits of their geographic range remain the same. Given their broad distributions, there was 100% overlap of both species and these 13 offshore wind projects. The

transmission cable routes of Sunrise Wind had the highest overlap area with both species' distributions. Maryland Offshore Wind Project had the lowest overlap area with *M. canis* distribution (Table 4), but *L. ocellata* spring and fall distributions shared the least overlap area with both Maryland Offshore Wind Project and Atlantic Shores Project 1 equally (Table 5).

**Table 4.** Square kilometers of Atlantic OWFs' cable route footprints intersecting with fall *M. canis* biomass across 2015-2019. Projects are ordered based on location south-to-north. Overlapping cable footprint area was calculated by multiplying the number of pixels containing cable and biomass ("count" column) by the pixel resolution (16km<sup>2</sup>) of the maps.

<b>Project Name</b>	<b>Electric Current</b>	<b>Status</b>	<b>(Expected) Operation Date</b>	<b>Count</b>	<b>Cable Route Footprint (km<sup>2</sup>)</b>
Kitty Hawk North	AC	proposed	2029	9	144
Coastal Virginia (commercial)	AC	proposed	2026	9	144
Coastal Virginia (pilot)	AC	proposed	2020	5	80
Maryland Offshore Wind Project	AC	proposed	2026	4	64
Ocean Wind	AC	cancelled	-	15	240
Atlantic Shores North	AC and/or DC	proposed	2027	11	176
Atlantic Shores South	AC and/or DC	proposed	2027	5	80
Empire Wind	AC	proposed	2027	12	192
South Coast Wind	TBD	proposed	2029	21	336
Vineyard Wind (VW1)	AC	proposed	2024	8	128
Sunrise Wind	DC	proposed	2026	22	352
South Fork Wind	AC	operating	2024	13	208
Revolution Wind	AC	proposed	2026	7	112
				<b>Total</b>	2,256

**Table 5.** Square kilometers of Atlantic OWFs’ cable route footprints intersecting with spring and fall *L. ocellata* biomass across 2015-2019. Projects are ordered based on location south-to-north. Overlapping cable footprint area was calculated by multiplying the number of pixels containing cable and biomass (“count” column) by the pixel resolution (16km<sup>2</sup>) of the maps.

Project Name	Electric Current	Status	(Expected) Operation Date	Count	Cable Route Footprint (km <sup>2</sup> )
Kitty Hawk North	AC	proposed	2029	9	144
Coastal Virginia (commercial)	AC	proposed	2026	9	144
Coastal Virginia (pilot)	AC	proposed	2020	5	80
Maryland Offshore Wind Project	AC	proposed	2026	4	64
Ocean Wind	AC	cancelled	-	15	240
Atlantic Shores North	AC and/or DC	proposed	2027	11	176
Atlantic Shores South	AC and/or DC	proposed	2027	4	64
Empire Wind	AC	proposed	2027	12	192
South Coast Wind	TBD	proposed	2029	21	336
Vineyard Wind (VW1)	AC	proposed	2024	8	128
Sunrise Wind	DC	proposed	2026	22	352
South Fork Wind	AC	operating	2024	13	208
Revolution Wind	AC	proposed	2026	7	112
				<b>Total</b>	2,240

### Assessment of Species Biomass Interactions

Due to its large lease area footprint, the transmission cables of Sunrise Wind had the highest overlap with fish biomass from fall *M. canis* and spring *L. ocellata* distributions (Figures 10, 11). The cable routes of South Fork Wind, South Coast Wind, and Empire Wind had the next highest overlap with fall *M. canis* (Figure 10) and spring and fall *L. ocellata* biomass (Figure 11). However, seasonality affected which projects overlapped *L. ocellata* habitat most, as fall *L. ocellata* biomass had the highest overlap with cables of South Fork Wind (Figure 11).

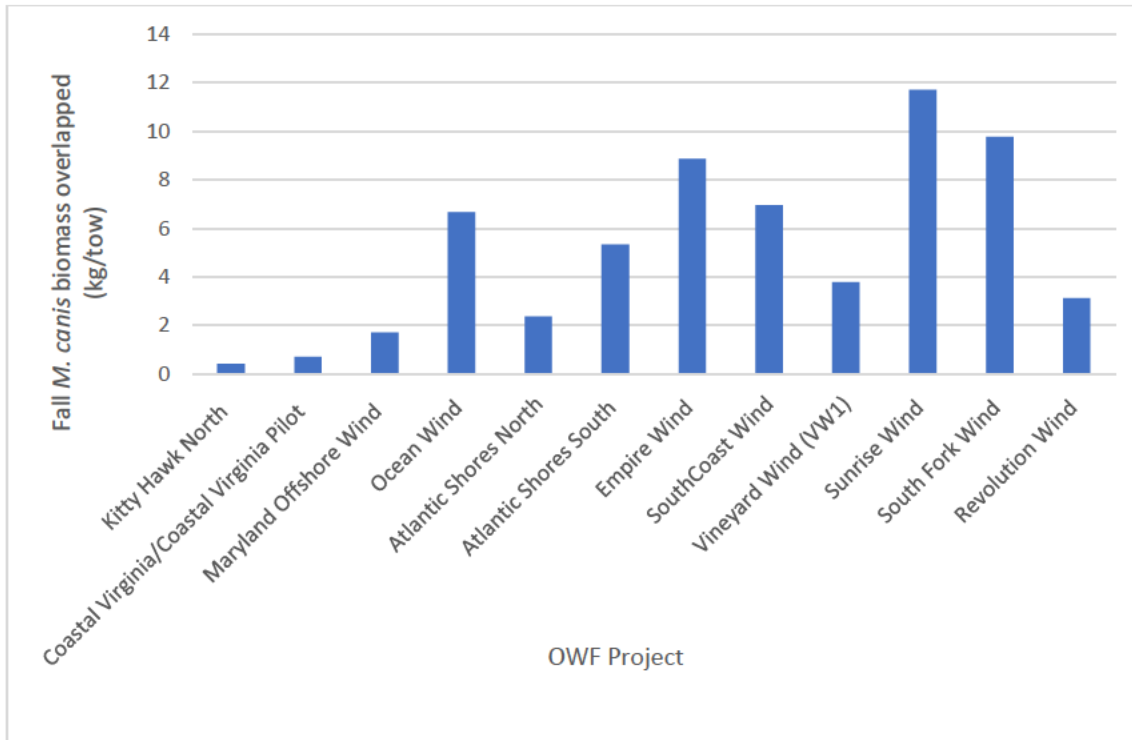


**Figure 10.** Overlap of fall *M. canis* biomass with each of the 13 OWF projects. Coastal Virginia commercial and pilot projects were combined into one project.

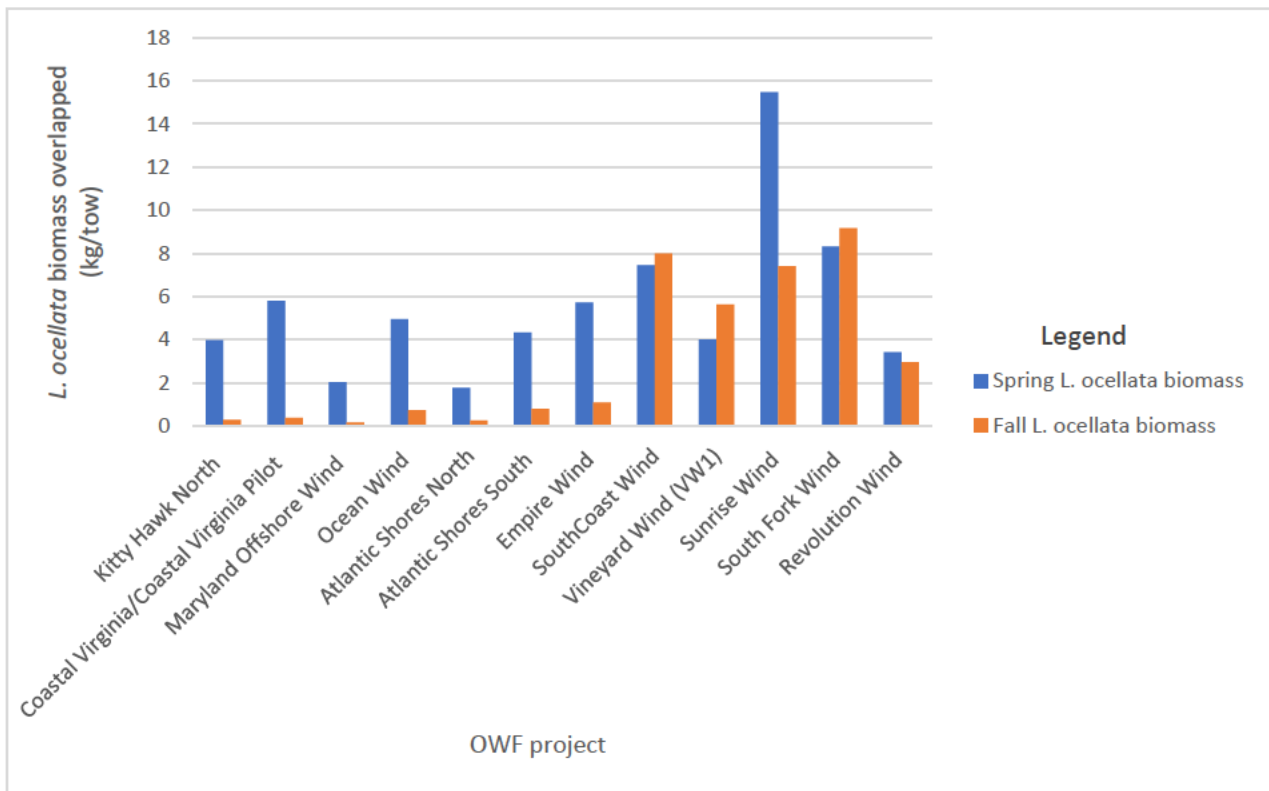


**Figure 11.** Overlap of spring and fall *L. ocellata* biomass with each of the 13 OWF projects' cable routes. Coastal Virginia commercial and pilot projects were combined into one project.

The proportions of *L. ocellata* biomass potentially impacted by offshore wind are very similar between spring and fall (10% and 8% respectively, Table 6), but fall biomass potential impacts were reduced in the lease areas related to the biomass shifts associated with seasonal movements (Figure 9). *Mustelus canis* biomass distribution showed a substantially higher percentage of biomass impacted by OWF, with greater overlap with cables than with lease areas (Table 6). During the fall season, nearly 27% of the *M. canis* study area biomass has the potential to be impacted by offshore wind, but more biomass is intersected by cable routes than by lease area (Table 6).

**Table 6.** Total proportions of seasonal species biomass (kg/tow) in contact with OWF cable routes and lease areas. The “Percent impacted by cables” row represents the proportion of study area biomass that was overlapping or intersecting cable routes. The “Percent impacted by lease area” row represents the proportion of study area biomass that was overlapping or intersecting lease areas. The “Total” row represents the combination of the previous calculations for cables and lease areas to illustrate the total proportion of the study population exposed to offshore wind.

	<b>Fall <i>M. canis</i></b>	<b>Spring <i>L. ocellata</i></b>	<b>Fall <i>L. ocellata</i></b>
Total biomass within cable routes (kg/tow)	61.47	67.29	36.88
Total biomass within lease areas (kg/tow)	42.91	79.03	35.56
Total study area biomass	389.75	1433.08	898.36
Percent impacted by cables	15.77%	4.70%	4.11%
Percent impacted by lease area	11.01%	5.51%	3.96%
<b>Total</b>	<b>26.78%</b>	<b>10.21%</b>	<b>8.06%</b>

## DISCUSSION

These results provide insight into the frequency that two benthic and demersal elasmobranch species may encounter EMFs from offshore wind transmission cables and lease areas. While possible dynamics between offshore wind lease area and fisheries has been covered in recent literature (Gill et al. 2020, Friedland et al. 2019, Friedland et al. 2023a,b), these results are a novel quantification of exposure to transmission cables specifically. The fall distribution of *M. canis* is concentrated more nearshore (Figure 7), which is also where OWF transmission cables and fixed turbine foundations are located. From 2015-2019, nearly 27% of the population biomass within the study area overlapped with and could be impacted by offshore wind. Of that 27% potentially impacted, nearly 16% is due to intersection with high-voltage transmission cables, while 11% is due to the intersection with lease area (Table 6). Therefore, the *M. canis* population in the region may be highly exposed to direct effects specifically from EMFs emitted by the cables, given that their physiological sensitivity to electric fields may be high based on the abundance of AOL pores (Figures 1, 2; Tables 1, 2). However, because *M. canis* is meso-pelagic or demersal, rather than benthic, and spends time swimming in the water column, exposure to EMFs is likely less direct and therefore possibly less impactful. The overlap between their habitat and OWF transmission cables is high, but an individual swimming in the water column may not actually encounter EMFs emitted by the cable.

During the study period, *L. ocellata* biomass inside the study area was higher than *M. canis* biomass (Table 6). Biomass totals more than 1400 kg/tow during the spring, but because a large percentage of it is offshore, the overall proportion intersected by offshore wind cable or lease area is lower than that of *M. canis* (Figure 8, Table 6). However, this does not necessarily mean that the species will not be impacted by offshore wind EMFs. While exposure may be

lower, winter skates are benthic and when they do come across a cable, they will be within two to three meters of the EMF, as this is how deep the cables are typically buried (NMFS 2020). While encounters may happen less frequently across the population, any skate that comes across the cable is very likely to detect its EMF and could have a behavioral response. Thus, exposure of spring and fall *L. ocellata* populations to OWF cables may still cause behavioral effects due to their proximity to the cables. *Leucoraja ocellata* are not known to migrate far north-to-south, but do undergo significant shifts horizontally during the spring and fall seasons. During the fall, *L. ocellata* distribution is densely aggregated offshore away from OWFs (Figure 9). Thus, seasonality plays a role in exposure level.

The geographic range of *M. canis* is similar to *L. ocellata*, but with a much higher degree of north-south migration (Conrath 2000). As a highly migratory species, *M. canis* migrates south during the fall or remains further north and hugs the shallow coastline (Conrath 2000). During the spring, they move north and slightly offshore, and were not caught by the trawl in high enough numbers inside the study area to include in this analysis. Thus, *M. canis* is likely primarily at risk of OWF interference during the fall season.

There is different reasoning behind potential impact from cable exposure and lease area exposure. A high proportion of biomass potentially impacted by cables routes of offshore wind suggests that impacts will be from EMFs. This could be in the form of attraction or repulsion (Hermans et al. 2024). Long-term studies should be done to analyze biomass exposure before and after long-term operation of a wind farm in order to support either case. However, due to the inability of elasmobranchs to differentiate artificial and biological electric fields, it is possible that curiosity may lead to an attraction influence as the cables' EMFs are misunderstood as potential prey (Kimber et al. 2011). While *M. canis* fall biomass in the study area is low relative

to winter skate biomass in both seasons, the sharks that are there are overlapping heavily in location with offshore wind cables routes (Figure 7). They were surveyed in higher densities close to the coastline as opposed to offshore like is displayed in the *L. ocellata* maps (Figure 8, 9). Due to the limitations of current technology, offshore wind farms are also restricted to this shallower shelf region. Thus, the significant potential (26% of the sample population biomass) for *M. canis* to be directly impacted by offshore wind in the Atlantic would almost certainly come from EMF exposure.

Unlike *M. canis* distribution, spring and fall *L. ocellata* distributions reflect that OWF lease areas are in areas of denser biomass than their cable routes, which may suggest that impacts to the species may come from the sounds and substrate of an operating offshore wind turbine in addition to EMFs. If behavioral responses such as attraction or repulsion occur, this would have major implications for the commercial *L. ocellata* fishery in the region. If skates are attracted to or displaced from the OWF locations, landings for the species will change. If attraction occurs, landings will decrease and the population may grow because commercial fishing is restricted in lease areas. In the case of an attraction response to EMFs, the fishery of the impacted species will be negatively impacted. Nearshore fixed wind turbines have the possibility to act as fish aggregating devices (FADs) and forage fish species have exhibited preference for areas within close proximity to offshore wind development (Fayram and De Risi 2007, Friedland et al. 2023b). Both examples demonstrate the artificial reef effect. If repulsion occurs, skates may move from restricted areas into harvesting regions and be subject to overfishing. Fishing pressure is often high directly outside of restricted lease areas (Fayram and De Risi 2007), meaning that catch rates may increase and sustainability of the fishery may be damaged. Both attraction and repulsion scenarios have been reported for elasmobranchs in the



literature (Kajiura and Fitzgerald 2009, Switzer and Meggitt 2010 and sources within, Tricas 2012, Friedland et al. 2021, Friedland et al. 2023b, Hermans et al. 2024, Newton et al. 2024).

Calculations of the proportion of each sample population exposed to offshore wind are confined to the limits of the trawl survey from which data were used. The geographic range of *M. canis* extends all the way down to Florida (Dell’Apa et al. 2018). Because a portion of their habitat is not within the area surveyed, the 26 percent calculated is really a proportion within a sample of the total population. If there were a trawl that surveyed at every square meter of a cable, the results of the analyses conducted here would likely be different. Finer scale data collection would be beneficial because biomass data, as well as presence-absence data of fish along the cable routes would be more accurate.

## CONCLUSIONS

Both *M. canis* and *L. ocellata* are designated as species with high exposure potential to OWF EMFs, but for different reasons. The high exposure of *M. canis* is due to its habitat overlap with offshore wind cables, with nearly 16% of the study population biomass located within transmission cable networks. *Mustelus canis* is demersal, but not benthic. So, this suggests that while the overlap is substantial between biomass and cable routes potentially impacting individuals, it is possible that interactions with EMFs may be limited to foraging. The majority of detection of EMFs by *M. canis* will likely come during feeding, which is done at or near the ocean floor. Exposure of *M. canis* to EMFs is high regarding geographic location relative to cables, but their proximity to the cables lowers direct encounters. High exposure of *L. ocellata* is due to its close proximity to the benthos. While the proportion of population biomass

is less for *L. ocellata* within these regions, their benthic life style places them in the direct vicinity of generated EMFs, potentially impacting their behavior, movement, and foraging.

The winter skate fishery is among the largest commercial fisheries in the northeast and makes up the most landings of any elasmobranch (NOAA 2023a). The growing smooth dogfish fishery is another crucial fishery to the northeastern U.S. Any potential distribution shifts caused by offshore wind development are extremely relevant for commercial fishers. The degree of exposure found in this study indicates that behavioral response from EMFs may be likely for both *M. canis* and *L. ocellata* populations. Being that other elasmobranchs have been unable to differentiate natural and artificial electric stimuli (Kajiura and Fitzgerald 2009, Kimber et al. 2011, Hutchison et al. 2020, Newton et al. 2024), further investigation with behavioral response studies should be conducted on both species.

The footprints of OWFs in the northeast will also alter the operation of several bottom trawl surveys important for stock assessments. Thus, offshore wind development will not only impact electro and magneto-sensitive marine animals directly, but will also impact our ability to survey affected species (Friedland et al. 2019, Friedland et al. 2023a). Large scale bottom trawl surveys will not be able to operate because of the spacing of the turbines and cable patterns. Additionally, while the use of smaller trawls by state agencies and acoustic telemetry may still be used, bottom trawl surveys serve as a crucial method of active fisheries sampling (Friedland et al. 2023a). All offshore wind companies are required to conduct their own surveys and monitoring plans via trawls, gillnetting, acoustic telemetry, and other methods (Methratta et al. 2023). Using similar strategies as those outlined in this project to calculate the percentage of species' population exposed to a project is a great way for OWF companies to quantify possible effects to marine life.

Offshore wind plans are also taking off on the west coast, and similar to the east coast, the effects to marine life have yet to be studied in depth. This project serves as a building block for research on the potential effects of offshore wind to vulnerable fishery species. This project is the first to numerically calculate the area of overlap specifically between the transmission cables of offshore wind and fish biomass. Knowledge of the proportion of a fish population that will potentially be impacted by the development of an offshore wind project may help in the lease area determination process. Additionally, this type of analysis gives insight into the species that should be a focus of further empirical research to test behavioral responses to EMFs and long-term OWF exposure. If both *exposure* to OWF cables and *sensitivity* to electric fields based on high AOL pore counts are high, then the species' *vulnerability* to impact from offshore wind development is high and should be studied further.

In conclusion, because so many planned and operating OWFs are clustered off the coasts of Massachusetts and Rhode Island, fish and elasmobranch species inhabiting this shallower, shelf region will all be prone to impacts, whether through attraction or repulsion. *Mustelus canis* and likely other demersal elasmobranchs that inhabit shallower waters of the coast and also have a well-developed electrosensory system can be considered of specific concern for behavioral effects from OWF EMFs. Relative to *M. canis*, a smaller proportion of *L. ocellata*'s population is affected. However, on an individual basis, effects to the winter skate will likely still be significant due strictly to their proximity to the cables as a benthic species.

## SUMMARY

To understand vulnerability, we must consider physiological sensitivity to or resolution of electric fields based on pore counts (Chapter 1) and spatial exposure to EMFs emitted by OWF transmission cable routes (Chapter 2). By evaluating sensitivity and potential exposure, we are able to categorize the smooth dogfish, *M. canis*, and the winter skate, *L. ocellata*, into a vulnerability category in Figure 12. *Mustelus canis* can be placed in the “high exposure and high sensitivity” category because its pore counts were high (1052 to 1924), indicating a high resolution electrosensory system (Tables 1, 2), and its spatial exposure to OWF transmission cables emitting EMFs was high (16% of the fall sample population). *Leucoraja ocellata* can be placed in the “high exposure and low sensitivity” category. Pore counts for *L. ocellata* were low (381 to 741), indicating a low resolution electrosensory system, and its biomass exposure to OWF transmission cables emitting EMFs was low (5% of spring sample population, 4% of fall sample population) as well. However, its proximity to transmission cables on the benthos increases its exposure to EMFs drastically from the “low” to “high” category. It should be noted once more that the “sensitivity” measure used here refers to resolution (abundance of AOL pores), whereas true sensitivity (longer canals and larger ampulla) may be determined for either species only through imaging techniques like diceCT and may change their placement on this diagram. High resolution does not necessarily equate to high sensitivity. The relationship between the two depends largely on age and foraging ecology and is species-specific. Species that rely heavily on electro-reception will likely be substantially more impacted by EMF than species that rely on visual cues. Notably, “vulnerability” as measured here is a spectrum. While *M. canis* was categorized as having high sensitivity and high exposure, its more distant proximity to cables likely causes them to fall somewhere in the middle of the true exposure spectrum.

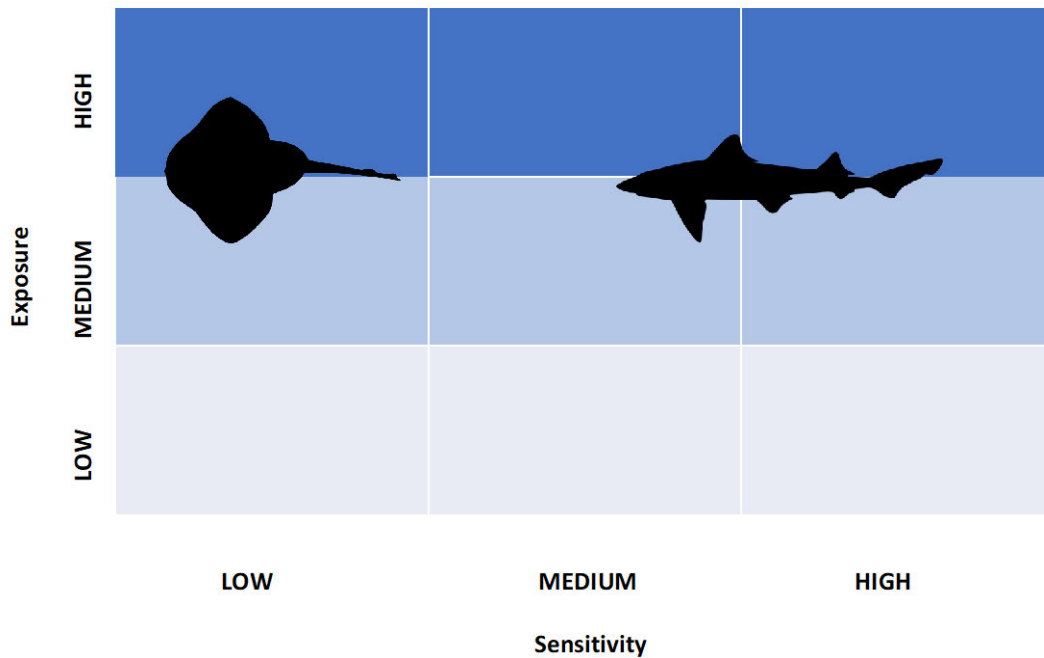


**Figure 12.** The spectrum of vulnerability to offshore wind EMFs based on the combination of physiological sensitivity and spatial exposure.

While 27, ten, and eight percent of fall *M. canis* and spring and fall *L. ocellata* biomass, respectively, may seem small, the economic impact of such a proportion could be substantial. If 27 percent of *M. canis* biomass potentially impacted by offshore wind EMFs across an average year equates to a 27 percent economic loss in the fishery, this would present a large issue. Likewise, if ten percent of spring *L. ocellata* biomass displaced by offshore wind equates to a ten percent increase in fishing mortality, overfishing will economically damage the future of the fishery. In the scenario that either species is attracted to EMF from transmission cables, they may move into OWF cable networks with fishing restrictions in place and thus be excluded from the fishery. This would decrease fisheries landings and revenue but increase population numbers. On the contrary, a repulsion response by either species may cause them to travel away from cables and into open fishing areas, thus increasing landings and revenue for the fishery. This could increase fishing mortality for the species and potentially lead to overfishing of the population.

Behavioral impacts are still unknown, however, until more empirical research is conducted on these two species.

This research is the first to make the connection between AOL morphology and offshore wind EMF location relative to elasmobranch habitat. Both the former and the latter hold important questions to reveal potential effects of offshore wind on marine species, but the combination of the two may provide bigger picture insights. This research is a useful steppingstone for uncovering which species may be impacted by offshore wind development, and therefore will direct empirical research on behavioral effects of EMFs on elasmobranch fishes. In order to better test whether pore counts change with ontogeny, future research should examine more individuals and size ranges to accomplish more robust pore counts. The density of OWF lease areas and cable networks in the northeastern Atlantic makes the fisheries of the region particularly susceptible to potential displacement. Offshore wind will undoubtedly continue to take off in the next few decades; therefore, it is critical that we account for the species and fisheries that are going to be most impacted by it. An increase in anthropogenic electric and magnetic stimuli in the marine environment is unavoidable, so it is crucial that research on the biology and physiology of the electro-sensory systems of affected fish continues. The implications of this research are vital when considering that anthropogenic changes to the marine environment will affect elasmobranchs' ability to forage, find mates, and migrate, which will affect the marine ecosystem as a whole. Offshore wind is a promising approach to grow renewable alternatives to fossil fuels, but the planning process should be carefully evaluated to mitigate long-term negative consequences on marine species. It is possible for a successful marine economy and green energy economy to coexist, but it requires an ecosystem-level approach.

## REFERENCES

- Anderson, J. M., Clegg, T. M., Véras, L. V., & Holland, K. N. (2017). Insight into shark magnetic field perception from empirical observations. *Scientific Reports*, 7(1), 11042.
- Bedore, C. N., & Kajiura, S. M. (2013). Bioelectric fields of marine organisms: voltage and frequency contributions to detectability by electroreceptive predators. *Physiological and Biochemical Zoology*, 86(3), 298-311.
- Bergström, L., Kautsky, L., Malm, T., Rosenberg, R., Wahlberg, M., Capetillo, N.A., and Wilhelmsson, D. (2014). Effects of offshore wind farms on marine wildlife—A generalized impact assessment. *Environmental Research Letters* 9(3):034012, <https://doi.org/10.1088/1748-9326/9/3/034012>.
- Boon, A., Caires, S., Wijnant, I. L., Verzijlbergh, R., Zijl, F., Schouten, J. J., & Kooten, T. (2018). The assessment of system effects of large-scale implementation of offshore wind in the southern North Sea. Technical Report Number: 11202792-002-ZKS-0006 p. 61. <https://doi.org/10.13140/RG.2.2.23113.60000>.
- Camilieri-Asch, V., Shaw, J. A., Yopak, K. E., Chapuis, L., Partridge, J. C., & Collin, S. P. (2020). Volumetric analysis and morphological assessment of the ascending olfactory pathway in an elasmobranch and a teleost using diceCT. *Brain Structure and Function*, 225(8), 2347-2375.
- Chaji, M., & Werner, S. (2023). Economic impacts of offshore wind farms on fishing industries: Perspectives, methods, and knowledge gaps. *Marine and Coastal Fisheries*, 15(3), e10237.
- Conrath, C. L. (2000). Population dynamics of the smooth dogfish, *Mustelus canis*, in the Northwest Atlantic. 93p. Dissertations, Theses, and Masters Projects. William & Mary. Paper 1539617761. <https://dx.doi.org/doi:10.25773/v5-m4zy-ek21>
- Crawford, L. M., Edelson, C. J., Hueter, R. E., & Gardiner, J. M. (2024). Behavioral electrosensitivity increases with size in the sandbar shark, *Carcharhinus plumbeus*. *Environmental Biology of Fishes*, 107(3), 257-273.
- Curtis, T.H. and Sosebee, K.A. (2015). Landings composition of the northeast U.S. skate, Rajidae, wing fishery and the effectiveness of prohibited species regulations. *Marine Fisheries Review*, 77(4), 1-8.
- Dell'Apa, A., Pennino, M. G., Bangley, C. W., & Bonzek, C. (2018). A hierarchical Bayesian modeling approach for the habitat distribution of smooth dogfish by sex and season in inshore coastal waters of the US Northwest Atlantic. *Marine and Coastal Fisheries*, 10(6), 590-605.

- Fayram, A. H., & De Risi, A. (2007). The potential compatibility of offshore wind power and fisheries: an example using bluefin tuna in the Adriatic Sea. *Ocean & Coastal Management*, 50(8), 597-605.
- Fishelson, L., & Baranes, A. (1998). Distribution, morphology, and cytology of ampullae of Lorenzini in the Oman shark, *Iago omanensis* (Triakidae), from the Gulf of Aqaba, Red Sea. *The Anatomical Record: an official publication of the American Association of Anatomists*, 251(4), 417-430.
- Friedland, K. D., Adams, E. M., Goetsch, C., Gulka, J., Brady, D. C., Rzeszowski, E., ... & Staudinger, M. D. (2023a). Forage fish species prefer habitat within designated offshore wind energy areas in the US Northeast Shelf ecosystem. *Marine and Coastal Fisheries*, 15(2), e10230. <https://doi.org/10.1002/mcf2.10230>
- Friedland, K. D., Boucher, J. M., Jones, A. W., Methratta, E. T., Morse, R. E., Foley, C., & Rago, P. J. (2023b). The spatial correlation between trawl surveys and planned wind energy infrastructure on the US Northeast Continental Shelf. *ICES Journal of Marine Science*, fsad167. <https://doi.org/10.1093/icesjms/fsad167>
- Friedland, K. D., Methratta, E. T., Gill, A. B., Gaichas, S. K., Curtis, T. H., Adams, E. M., ... & Brady, D. C. (2021). Resource occurrence and productivity in existing and proposed wind energy lease areas on the Northeast US Shelf. *Frontiers in Marine Science*, 8, 629230.
- Gill, A. B., Degraer, S., Lipsky, A., Mavraki, N., Methratta, E., & Brabant, R. (2020). Setting the context for offshore wind development effects on fish and fisheries. *Oceanography*, 33(4), 118-127.
- Gill, A. B., Huang, Y., Gloyne-Philips, I., Metcalfe, J., Quayle, V., Spencer, J., & Wearmouth, V. (2009). COWRIE 2.0 Electromagnetic Fields (EMF) Phase 2: EMF-sensitive fish response to EM emissions from sub-sea electricity cables of the type used by the offshore renewable energy industry. *Commissioned by COWRIE Ltd (project reference COWRIE-EMF-1-06)*, 68.
- Gill, A. B., Huang, Y., Spencer, J., & Gloyne-Philips, I. (2012). Electromagnetic fields emitted by high voltage alternating current offshore wind power cables and interactions with marine organisms. In *Electromagnetics in Current and Emerging Energy Power Systems Seminar*. London, UK. COWRIE.
- Haine, O. S., Ridd, P. V., & Rowe, R. J. (2001). Range of electrosensory detection of prey by *Carcharhinus melanopterus* and *Himantura granulata*. *Marine and Freshwater Research*, 52(3), 291-296.
- Hermans, A., Winter, H. V., Gill, A. B., & Murk, A. J. (2024). Do electromagnetic fields from subsea power cables effect benthic elasmobranch behaviour? A risk-based approach for the Dutch Continental Shelf. *Environmental Pollution*, 123570. <https://doi.org/10.1016/j.envpol.2024.123570>



- Haueisen, M. and Reis, R.E. (2023). High resolution in turbid waters: Ampullae of Lorenzini in the daggenose shark *Carcharhinus oxyrhynchus*. *Journal of Fish Biology*. <https://doi.org/10.1111/jfb.15583>
- Hutchison, Z. L., Gill, A. B., Sigray, P., He, H., & King, J. W. (2020). Anthropogenic electromagnetic fields (EMF) influence the behaviour of bottom-dwelling marine species. *Scientific Reports*, *10*(1), 4219.
- Hutchison, Z. L., Gill, A. B., Sigray, P., He, H., & King, J. W. (2021). A modelling evaluation of electromagnetic fields emitted by buried subsea power cables and encountered by marine animals: considerations for marine renewable energy development. *Renewable Energy*, *177*, 72-81.
- Kajiura, S. M. (2001). Head morphology and electrosensory pore distribution of carcharhinid and sphyrnid sharks. *Environmental Biology of Fishes*, *61*, 125-133.
- Kajiura, S. M., & Fitzgerald, T. P. (2009). Response of juvenile scalloped hammerhead sharks to electric stimuli. *Zoology*, *112*(4), 241-250.
- Kalmijn, A.J. (1971). The electric sense of sharks and rays. *Journal of Experimental Biology*. *55*(2), 371-383.
- Kalmijn, A.J. (1982). Electric and magnetic field detection in elasmobranch fishes. *Science* *218*:916–918.
- Kempster, R. M., McCarthy, I. D., & Collin, S. P. (2012). Phylogenetic and ecological factors influencing the number and distribution of electroreceptors in elasmobranchs. *Journal of Fish Biology*, *80*(5), 2055-2088.
- Kimber, J.A., Sims, D.W., Gill A.B. (2011). The ability of benthic elasmobranchs to discriminate between biological and artificial electric fields. *Marine Biology*. 158:1-8.
- Kulka, D. W., Anderson, B., Cotton, C. F., Derrick, D., Pacoureaux, N., & Dulvy, N. K. (2020). *Leucoraja ocellata*. *The IUCN Red List of Threatened Species 2020: e.T161631A124518400*.
- Lauria, S., Schembari, M., Palone, F., & Maccioni, M. (2016). Very long distance connection of gigawatt-size offshore wind farms: extra high-voltage AC versus high-voltage DC cost comparison. *IET Renewable Power Generation*, *10*(5), 713-720.
- Methratta, E. T., Hawkins, A., Hooker, B. R., Lipsky, A., & Hare, J. A. (2020). Offshore wind development in the northeast US shelf large marine ecosystem. *Oceanography*, *33*(4), 16-27.
- Methratta, E. T., Silva, A., Lipsky, A., Ford, K., Christel, D., & Pfeiffer, L. (2023). Science priorities for offshore wind and Fisheries research in the northeast US Continental shelf

- ecosystem: perspectives from scientists at the National Marine Fisheries Service. *Marine and Coastal Fisheries*, 15(3), e10242. <https://doi.org/10.1002/mcf2.10242>
- Montemarano, J. J., Havelin, J., & Draud, M. (2016). Diet composition of the smooth dogfish (*Mustelus canis*) in the waters of Long Island, New York, USA. *Marine Biology Research*, 12(4), 435-442.
- Musial, W., Heimiller, D., Beiter, P., Scott, G., & Draxl, C. (2016). 2016 Offshore Wind Energy Resource Assessment for the United States. Golden, CO, USA. National Renewable Energy Laboratory. Report NREL/TP-5000-66599. <https://www.nrel.gov/docs/fy16osti/66599>
- Musial, W., Spitsen, P., Duffy, P., Beiter, P., Shields, M., Mulas Hernando, D., ... & Sathish, S. (2023). Offshore Wind Market Report: 2023 Edition. Golden, CO, USA. National Renewable Energy Laboratory. Report NREL/TP-5000-87232. (NREL), <https://doi.org/10.2172/2001112>
- Newton, K. C., Donato, N. H., Henkel, S., & Chapple, T. K. (2024). The Effects of Anthropogenic Electromagnetic Fields on the Behavior of Geomagnetically Displaced Skates. *bioRxiv*, 2024-04.
- Newton, K.C., Gill, A.B., & Kajiura, S.M. (2019). Electroreception in marine fishes: chondrichthyans. *Journal of Fish Biology*, 95:135-154.
- NMFS (2020). National Marine Fisheries Service. Fisheries Economics of the United States 2020. US Department of Commerce, NOAA Technical Memorandum NMFS-F/SPO-236A.
- NOAA (2023a). National Oceanic and Atmospheric Administration. 2022 Status of Stocks Report to Congress. U.S. Department of Commerce. Retrieved from <https://www.fisheries.noaa.gov/s3/2023-04/2022-Status-of-Stocks-RtC-041423-0.pdf>
- NOAA (2023b). National Oceanic and Atmospheric Administration. Atlantic Highly Migratory Species (HMS) Stock Assessment and Fishery Evaluation (SAFE) Report, 2022.
- Poscai, N. A. (2016). Estudo comparativo da morfologia dos nervos da linha lateral e ampolas de Lorenzini de *Rhizoprionodon lalandii* (Müller & Henle 1839) (tubarão-frango) e *Prionace glauca* (Linnaeus, 1758) (tubarão-azul) (Elasmobranchii:Carcharhinidae) [Comparative study of the lateral line and ampullae of Lorenzini nerves morphology of *Rhizoprionodon lalandii* (Müller & Henle 1839) (Brazilian Sharpnose Shark) and *Prionace glauca* (Linnaeus, 1758) (Blue Shark) (Elasmobranchii: Carcharhinidae).]. Dissertação apresentada ao Programa de Pós- Graduação em Anatomia dos Animais Domésticos e Silvestres da Faculdade de Medicina Veterinária e Zootecnia da Universidade de São Paulo. 70p.
- Raschi, W. (1986). A morphological analysis of the ampullae of Lorenzini in selected skates (Pisces, Rajoidei). *Journal of Morphology*, 189(3), 225-247.

- Raschi, W., & Adams, W. H. (1988). Depth-related modifications in the electroreceptive system of the eurybathic skate, *Raja radiata* (Chondrichthyes: Rajidae). *Copeia*, 116-123.
- Roundtree, R. A. (1996). Dogfish, *Mustelus canis*, in a New Jersey estuary. *Fishery Bulletin*, 94, 522-534.
- Saidi, B., Enajjar, S., Bradai, M. N., & Bouain, A. (2009). Diet composition of smooth-hound shark, *Mustelus mustelus* (Linnaeus, 1758), in the Gulf of Gabès, southern Tunisia. *Journal of Applied Ichthyology*, 25, 113-118.
- Seelye, K. Q., & Salem, N. (2014). Even Before Long Winter Begins, Energy Bills Send Shivers in New England. *NY Times* (Dec. 13, 2014), <http://www.nytimes.com/2014/12/14/us/even-before-long-winter-begins-energy-bills-send-shivers-in-new-england.html>.
- Skjæraasen, J. E., & Bergstad, O. A. (2000). Distribution and feeding ecology of *Raja radiata* in the northeastern North Sea and Skagerrak (Norwegian Deep). *ICES Journal of Marine Science*, 57(4), 1249-1260.
- Switzer, T., & Meggitt, D. (2010). Review of literature and studies on electro magnetic fields (EMF) generated by undersea power cables and associated influence on marine organisms. *OCEANS 2010 MTS/IEEE SEATTLE*, 1-5.
- Szczepanski, J. A. (2013). Feeding ecology of skates and rays in Delaware and Narragansett Bays. Open Access Dissertations. Paper 27. 199p. [https://digitalcommons.uri.edu/oa\\_diss/27](https://digitalcommons.uri.edu/oa_diss/27)
- Tricas, T. (2012). Effects of EMFs from undersea power cables on elasmobranchs and other marine species (Report No. BOEMRE 201109). Report by Normandeau Associates Inc. Report for Bureau of Ocean Energy Management (BOEM) and the US Department of the Interior (DOI).
- Zhang, X., Xia, K., Lin, L., Zhang, F., Yu, Y., St. Ange, K., ... & Linhardt, R. J. (2018). Structural and functional components of the skate sensory organ ampullae of *Lorenzini*. *ACS Chemical Biology*, 13(6), 1677-1685.
- Zhang, J., Zheng, X. L., Chen, G. Z., Zhang, Z. G., & Xu, B. B. (2014). Economic Comparison of VSC-HVDC and HVAC Systems for Connections of Offshore Wind Farms. *Applied Mechanics and Materials*, 672, 325-330.

### External Data Sources

BOEM shapefiles:

BOEM Offshore Wind - Export Cable Locations (2024) [downloaded shapefile]. Northeast Ocean Data, Esri. Accessed by Rachel Sechrist [05/06/24].

URL: <https://www.boem.gov/sites/default/files/documents/renewable-energy/state-activities/Atlantic%20OCS%20Renewable%20Energy%20Lease%20Areas.pdf>